

Macrofauna abundance, species diversity and turnover at three sites in the Clipperton-Clarion Fracture Zone

George D. F. Wilson¹

Received: 4 June 2016 / Revised: 13 November 2016 / Accepted: 15 November 2016 / Published online: 9 December 2016
© Senckenberg Gesellschaft für Naturforschung and Springer-Verlag Berlin Heidelberg 2016

Abstract The fauna of three sites in the Clipperton-Clarion Fracture Zone Region of the North Pacific Ocean were evaluated as part of multiple programs supported by the US National Oceanic and Atmospheric Administration. These localities (Site A in the west and Site C and a prospective reserve area 2893–2561 km to the east) cover the range of depths and productivity observed for the region. Macrofauna densities varied with productivity, with Site A with the lowest densities and the reserve area with the highest densities. Species diversities of Polychaeta, Isopoda and Tanaidacea showed differing trends compared to export productivity, using a bootstrapped lognormal method to estimate total species. Polychaeta had the highest estimated species at the high-productivity reserve site and the lowest values at the low-productivity site A. Tanaidacea had a similar trend to that of the polychaetes. Isopoda showed an opposite species–productivity trend, with highest estimated species at the low-productivity site A and lowest values at the high-productivity reserve site. Polychaetes were most similar between sites, while isopod similarities were low. Tanaid similarities between sites A and C resembled the polychaetes value. Species turnover for isopods was high, but much less so for polychaetes and tanaids, and may be related to the dispersal potential for each taxocene. Beta diversity predicts that the average isopod species in the CCFZ has a range of approximately

2200 km² while a polychaete species range might exceed 10,000 km². Data from a single taxocene cannot be used as a proxy for the entire deep-sea fauna because each group has its own ecological and evolutionary responses, as well as its own history.

Keywords Abyssal benthos · Polychaeta · Isopoda · Tanaidacea · Beta diversity · Species richness

Introduction

Recent interest in the deep sea of the Clipperton-Clarion Fracture Zone derives from the potential mineral wealth residing in manganese nodules (Martino and Parson 2012; Hein et al. 2013). During the period 1970–1992, the USA National Oceanic and Atmospheric Administration (NOAA) sponsored multiple research projects in the CCFZ to document the habitats and fauna, and to understand impacts on deep-sea assemblages that might be caused by mining (Hecker and Paul 1979; Jumars 1981). Bischoff and Piper (1979) report on the NOAA Deep Ocean Mining Environmental Study (DOMES) conducted during the early part of the 1970s decade. Later projects (Jumars 1980, 1981; Spiess et al. 1984; Wilson and Hessler 1987; Wilson 1990a, b, c, 1992) provided data that are presented in this paper. This paper provides a comparative overview of the macrofauna collected during these latter studies and assesses the species diversity and faunal similarity across the three sites. Sea floor images from a typical CCFZ site (14°40'N, 126°25'W, depth 4500 m) are shown in Fig. 1. Because together the three sites span much of the distance and productivity range present in the CCFZ, they provide a starting point for future research on this huge region of the abyssal sea floor. An effort has been made to find and standardize all available faunal data that have only appeared in government reports, some of which have been

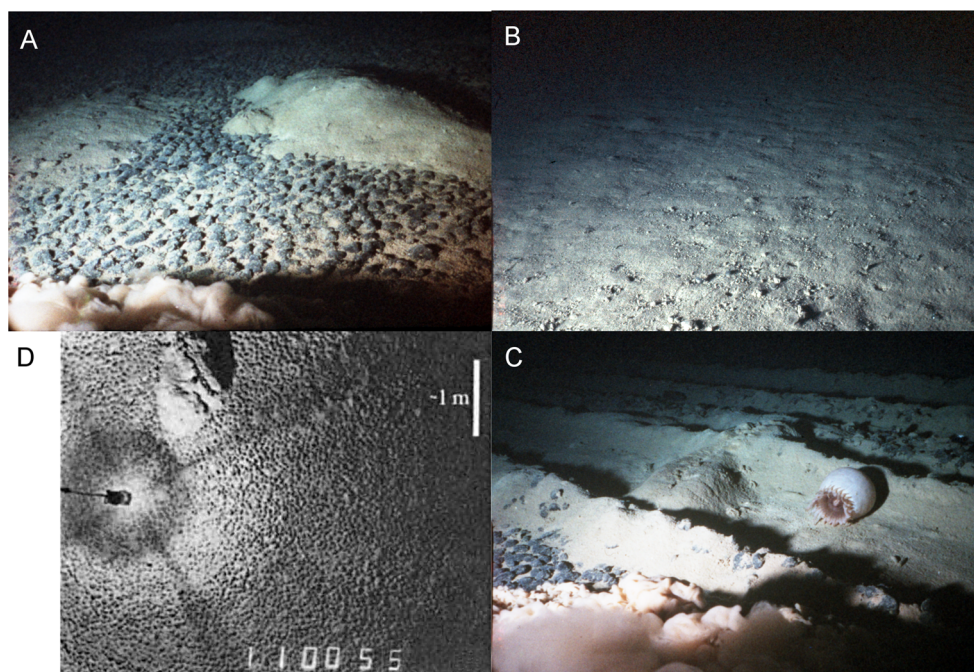
Communicated by S. S. M. Kaiser

Electronic supplementary material The online version of this article (doi:10.1007/s12526-016-0609-8) contains supplementary material, which is available to authorized users.

✉ George D. F. Wilson
gdfw@snhlab.com

¹ Saugatuck Natural History Laboratory, P O Box 714, Saugatuck, MI 49453, USA

Fig. 1 Seafloor images taken near 14°40'N, 126°25'W, depth 4500 m. **a, b, c** Images taken by RUMIII (Wilson 1990a), showing the range of bottom types. A decades-old mining track is shown in **c**. **d** Image taken by Deep-Tow during Cruise ECHO I (Spiess et al. 1984; de Moustier 1985)



unavailable prior to this time. Partial data from these studies have appeared in other reports (Cunha and Wilson 2003; Glover et al. 2002; Mullineaux 1987, 1988a, b, 1989; Paterson et al. 1998; Riehl et al. 2014; Thistle and Wilson 1987, 1996; Spiess et al. 1984; Spiess, and Weydert 1987; Wilson and Hessler 1987; Wilson 1987a, b, 1990a, b, 1992).

These programs were designed to evaluate the impact of manganese nodule mining (Jumars 1981; Morgan et al. 1999; Glover and Smith 2003). For multiple reasons, our results were equivocal on how nodule mining might change fragile abyssal assemblages (Jumars 1977, 1980, 1981; Wilson and Hessler 1987). We observed that physical impacts such as miner tracks that persisted for decades (Spiess et al. 1984; Wilson 1990a; Fig. 1c). Because the nodules themselves take millennia to grow (Knoop et al. 1998), and because the fauna of the CCFZ is adapted to a low sedimentation rate, one might predict that recovery after mining will take a decades, centuries or longer (Jumars 1981; Glover and Smith 2003; Miljutin et al. 2011). Given this background, these data are presented to provide a benchmark for our knowledge of three locations and different taxocenes in this vast abyssal region. The data show that the faunal densities correlate well with surface and export productivity, but not diversities and species turnover for each group. Different taxocenes, Polychaeta and Isopoda in this case, show substantially different responses to the environment of the CCFZ.

Environmental setting

The Clipperton-Clarion Fracture Zone (CCFZ) is bounded longitudinally by 120°–160°W and encompasses a huge area ($5.1 \times 10^6 \text{ km}^2$) in the North Pacific Ocean, south and east of

Hawaii. This area is characterized by a gradual deepening toward the west so that the eastern margin is around 4000 m deep, while south of Hawaii depths exceed 5000 m (Piper et al. 1979a, b). At 10-km scales, the seafloor varies over a 200-m depth range owing to “abyssal hills” that trend in a north–south direction, created at the Eastern Pacific Rise during the generation of new seafloor crust (Craig 1979; Mudie et al. 1972). This topography contributes to variation in the distribution of manganese nodules at all sites (Craig 1979). As sediments become deeper to the west, the topography becomes more moderated (Piper et al. 1979a, b), with different ridge and valley patterns (e.g., Piper and Blueford 1982). Because most sites are below the calcite compensation depth, sediment in this region contains little or no calcareous debris.

DOMES site A

Site A is in the north Equatorial Pacific centered on 9°24'N, 151°27'W. An east–west trending valley with a depth range 4900–5200 m is the main topographic feature. The trend of the valley and rough north–south ridges of the highlands indicate that it may represent a fracture zone (Piper and Blueford 1982). The sediments contain siliceous clays with a mean clay content of 50%, the remainder being primarily siliceous ooze (Piper et al. 1979a). The highlands, covered by Quaternary sediment, are areas of deposition. Along the north margin of the valley, nodules and sediment resemble those of the highlands (Piper et al. 1979a). Early Tertiary sediment outcrops at the surface of the south margin of the valley were interpreted as ongoing erosion, perhaps by Antarctic Bottom Water flows (Piper et al. 1979a). The near-bottom daily-averaged current

velocities were 2 cm/s. The average flow was to the north-west at 0.45 cm/s, with some low-frequency fluctuations having periods from 2 to 5 months (Hayes 1979). At similar sites to the east (11°N, 140°W), long-term seafloor observations for up to 3 years did not detect current velocities sufficiently strong to generate shear stresses capable of re-suspending sediments (Gardner et al. 1984). Stratigraphic data show that episodes of sediment erosion and redeposition took place as late as the Pleistocene (Piper et al. 1979a). The erosional events are associated with seabed current intensification during glaciation (Johnson 1972; Quinterno and Theyer 1979). The near-bottom water has salinities of 34.68 to 34.69‰ and temperatures of 1.4 ± 0.004 °C (Hayes 1979). In 1978, site A was subjected to test mining for manganese nodules (Lavelle et al. 1981), with benthic sampling before and after the event (Jumars 1980; Lavelle et al. 1981; Fig. 2). Manganese nodule cover typically varied between 10 and 25%, with some samples lacking nodules altogether (Piper and Blueford 1982). Mean nodule abundances were approximately 253 m², ranging from 2 to 495 in a sample (estimated from data in Piper and Blueford 1982).

DOMES site C

Site C is also referred to as ECHO I locality, because samples were taken on the first leg of the Scripps Institution of Oceanography (SIO) campaign ECHO (Spiess et al. 1984). The location of the Ocean Management Incorporated (OMA) test mining and the 1983 ECHO I sampling program was 14°40'N, 126°25'W at a depth of 4500 m (Figs. 1, 3). This site lies between the Clipperton and Clarion fracture zones, 2000 km to the west of the Eastern Pacific Rise and is near DOMES site C (15°N, 125°W). The temperatures, salinities, and current regime are similar to that at site A (Hayes 1979). The sediments are transitional between pelagic red clay and siliceous ooze, with generally dark yellowish-brown Quaternary sediments at the surface (Spiess et al. 1984). The bathymetry, determined from a Sea Beam survey (de Moustier 1985), shows abyssal hills trending north–south. The study site was on a relatively flat area with gentle slopes to the east, and surrounded by depressions on the east and the west (de Moustier 1985; Spiess and Weydert 1987). During 1978, OMA programs at the ECHO I locality disturbed the seafloor with various versions of a wire-towed sled or a prototype mining vehicle (Spiess and Weydert 1987). Active pumping

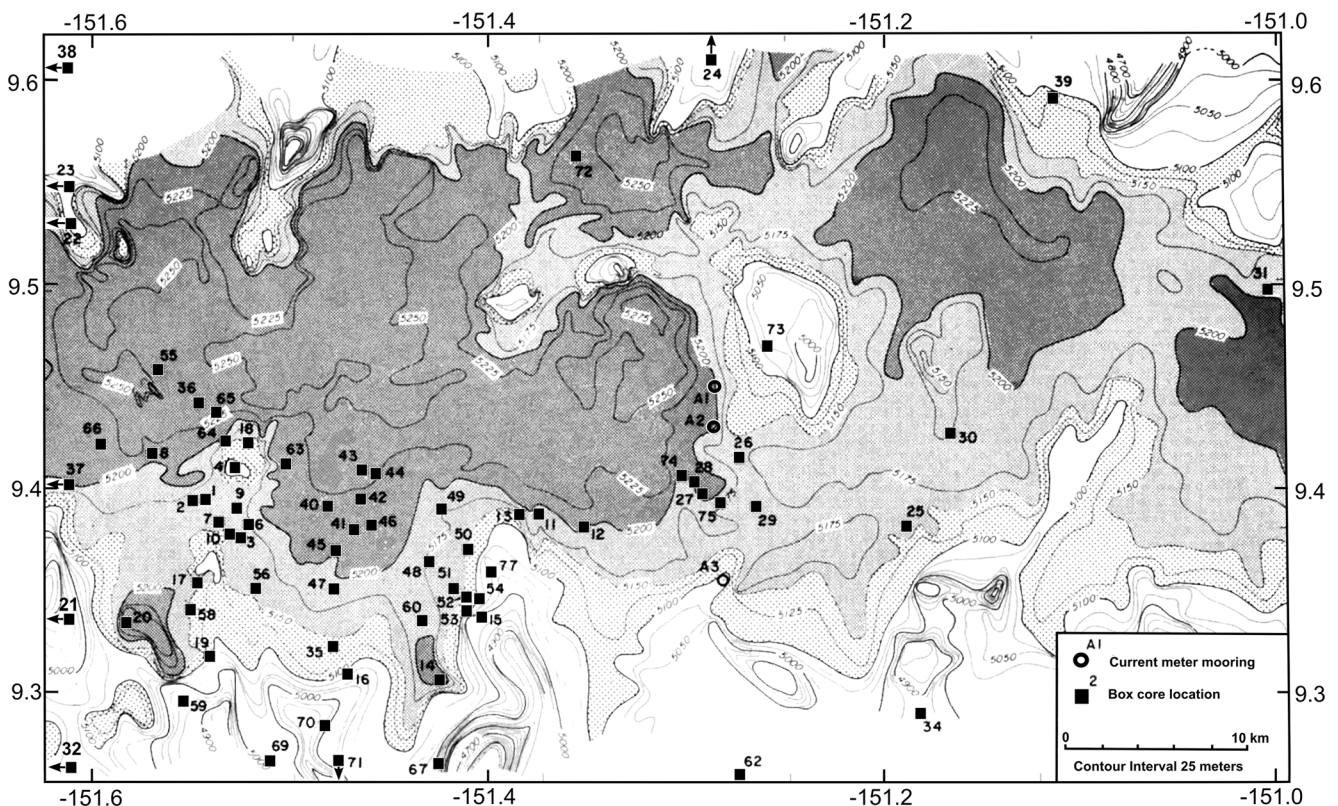
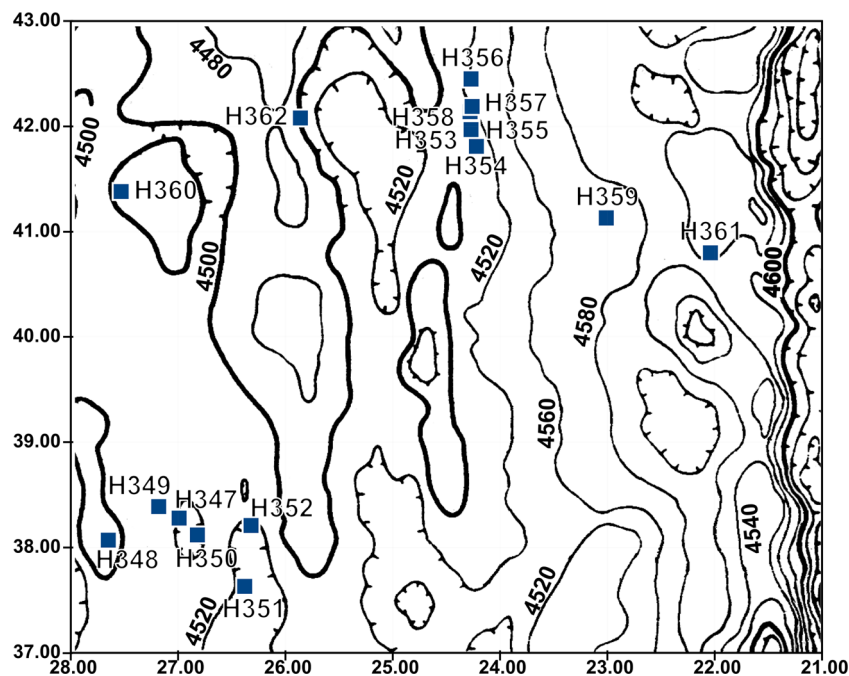


Fig. 2 Domes site A, approximate positions of samples and topography, modified from Piper and Blueford 1982, who withheld the precise locality data on request from a mining company. Figure positions were correlated with actual sample positions in Table 1, and the map axes

corrected to real world positions. Sample positions are indicative and not precise. Samples from both 1977 and 1978 cruises are shown, although several samples were outside the area of the map and are indicated by a sample marker and arrow

Fig. 3 DOMES site C, positions of sample sites superimposed on topographic map from Spiess et al. (1984). See Table 1 for precise positions



of nodules from the seafloor and generation of a sediment plume occurred only during a few occasions and primarily during a November–December 1978 OMA/DSV cruise on the R/V *Deepsea Miner II* (Dick and Foell 1985). Probably owing to the low frequency of the pumping, Wilson and Hessler (1987) found no detectable effects of the test mining disturbance on the benthic fauna. Therefore, the data from this study are assumed to be more or less representative of the general benthic community in the ECHO I (site C) locality. Manganese nodules are the dominant feature of the sedimentary surface at the ECHO I site (Spiess and Weydert 1987) with coverages of 25–49% in the box corer samples (Wilson and Hessler 1987), with average long axial lengths ranging from 5.0 to 6.75 cm (Spiess and Weydert 1987). Photographic surveys using the Deep-Tow vehicle (Spiess and Weydert 1987) and acoustic reflectivities derived from Sea Beam surveys (de Moustier 1985) show that nodule coverages can range from 0 to 80% in this general area. The average nodule size (expressed as cm^2) shows a significant inverse relationship with the nodules density ($R = -0.96$) at the sampling scale of 0.25 m^2 (Wilson and Hessler 1987).

Preservational reserve area site (PRA)

The PRA Site (NOAA designated “Provisional Interim Protected Reserve Area”) is a region that was to be set aside and excluded from mining, as a stable reference area (Wilson 1990a). The site was not known to be subjected to mining impacts by the time it was sampled in 1989. The PRA site is a typical abyssal hills region of the Central Pacific (Wilson 1990a; Fig. 4) with sampling centered on $12^\circ 57' \text{N}$ $128^\circ 20' \text{W}$, 4794 m (Fig. 5). The topography of the study area consists of a typical low relief abyssal hill complex with ridges arranged on approximately north–south

axes (4700–4900 m). Mean temperatures at the site were 1.48°C and water movement in the region has a mean velocity of 3.23 (range 0.9–1 3.4) cm/s, with average flow toward the northeast. This current also has a well-defined tidal component that was oscillatory (D. Pillsbury, personal communication; unpublished NOAA report 1991). The bottom type has an approximately similar sedimentary facies as ECHO I samples H359 and H361, but showing higher water content in the surface light brown silicate and silt clays in all samples. A horizon at c. 10 cm was observed in one sample (PRA17) below which the sediments became coarse, semi-consolidated, and gray, similar to the discontinuity caused by the presence Tertiary sediments observed at the other sites. The higher water content of the sediments resulted in deep penetration of the sampler on several occasions. Nodule cover was fairly low, less than 10% cover in most cases, averaging 23.3 nodules/ m^2 . Samples this site contained 0–36 nodules, most of which had diameters less than 5 cm. Several samples had single large, granular nodules as large as 25 cm in diameter. These densities were lower than those observed at the ECHO I locality, which averaged 274.3 nodules/ m^2 , although the PRA nodules were much larger on the average.

Materials and methods

Sample collection and processing

Table 1 has the locality data for all sites, which were sampled using different versions of the 0.25-m^2 box corer, initially designed by R.R. Hessler, Scripps Institution of Oceanography. This paper considers only the macrofauna, those members of the

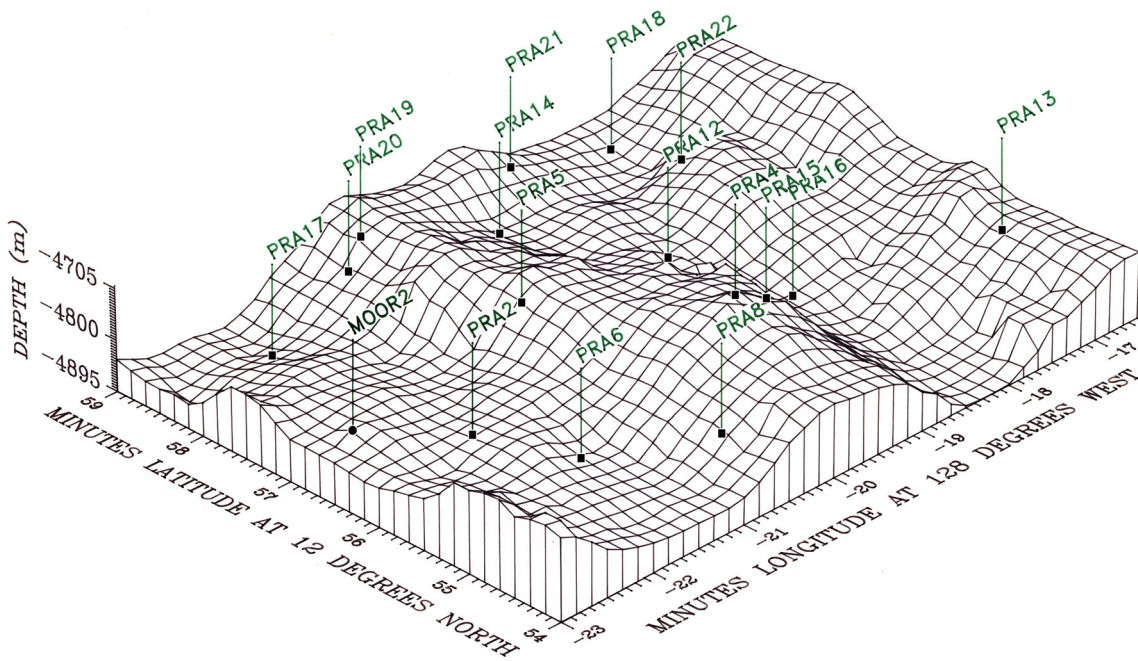


Fig. 4 PRA site, geomorphology with sample positions (see Table 1). Topography derived from depth-sounding survey data taken during sampling

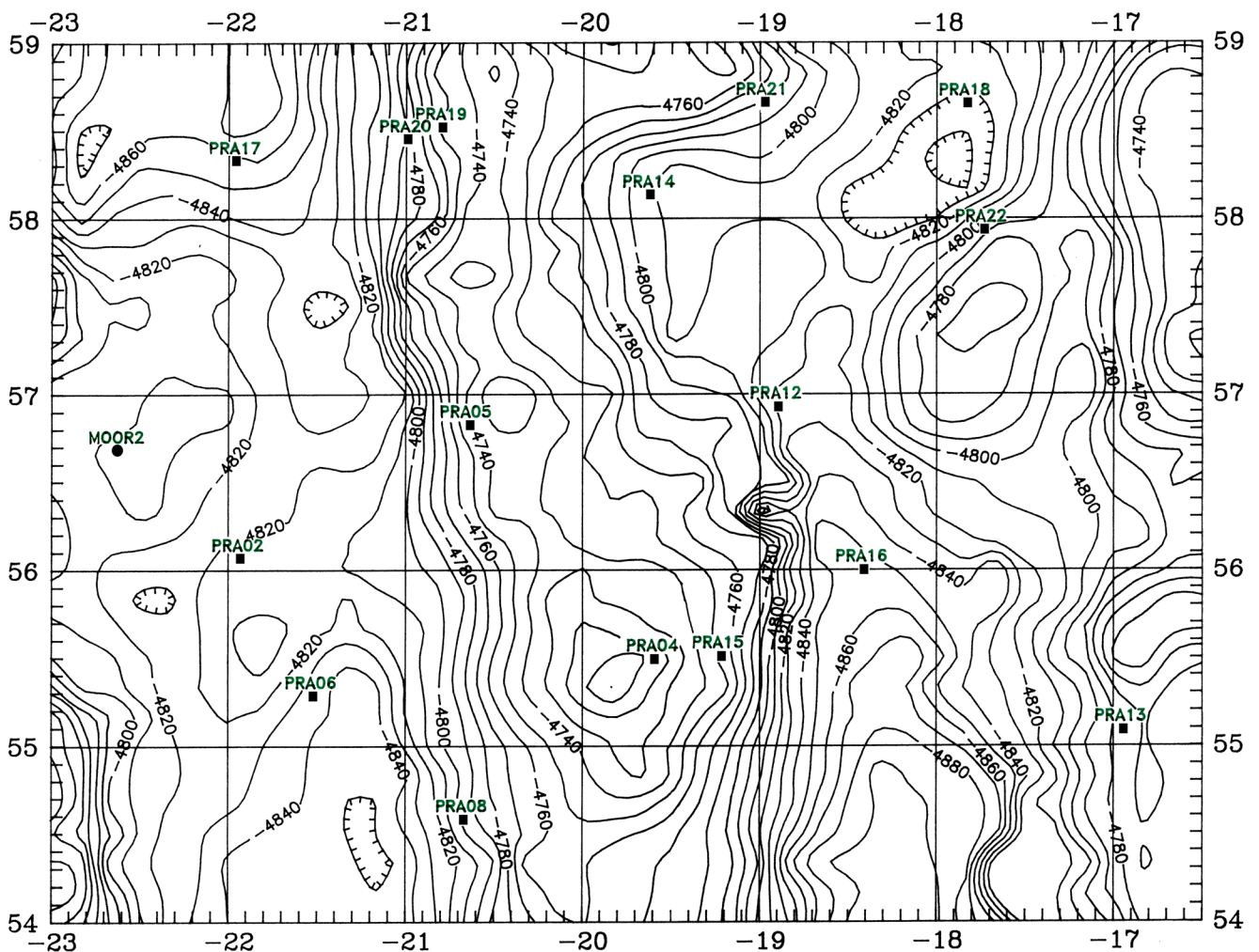


Fig. 5 PRA site, topography with sample positions (see Table 1). Map scale in minutes of latitude at 12°N and 128°W

Table 1 Samples from three sites in the Clipperton-Clarion Fracture Zone

PROGRAM	Sample	Date	POSITION	Depth (m)	Sampler
DOMES #1	DJ02	11/22/1977	9°23.51'N, 151°32.94'W	5155	BC,SANDIA
DOMES #1	DJ07	11/23/1977	9°22.93'N, 151°32.04'W	5170	BC,SANDIA
DOMES #1	DJ08	11/24/1977	9°25.23'N, 151°34.46'W	5205	BC,THIEL
DOMES #1	DJ10	11/24/1977	9°22.81'N, 151°31.83'W	5183	BC,THIEL
DOMES #1	DJ11	11/25/1977	9°23.5'N, 151°22.5'W	5174	BC,THIEL
DOMES #1	DJ12	11/25/1977	9°22.9'N, 151°20.6'W	5187	BC,THIEL
DOMES #1	DJ13	11/25/1977	9°23.3'N, 151°23'W	5187	BC,THIEL
DOMES #1	DJ15	11/26/1977	9°20.3'N, 151°24.1'W	5166	BC,THIEL
DOMES #1	DJ16	11/26/1977	9°18.6'N, 151°28.5'W	5120	BC,THIEL
DOMES #1	DJ18	11/26/1977	9°25.6'N, 151°31.2'W	5160	BC,THIEL
DOMES #1	DJ20	11/27/1977	9°19.8'N, 151°35.1'W	5260	BC,THIEL
DOMES #1	DJ21	11/27/1977	9°20.5'N, 151°45'W	5203	BC,THIEL
DOMES #1	DJ22	11/28/1977	9°32.4'N, 151°39.1'W	4908	BC,THIEL
DOMES #1	DJ23	11/28/1977	9°33.23'N, 151°38.33'W	4934	BC,THIEL
DOMES #1	DJ24	11/28/1977	9°31.2'N, 151°17.1'W	5164	BC,THIEL
DOMES #1	DJ25	11/28/1977	9°22.64'N, 151°12.28'W	5177	BC,THIEL
DOMES #1	DJ26	11/29/1977	9°24.82'N, 151°16.42'W	5170	BC,THIEL
DOMES #1	DJ28	11/29/1977	9°24.12'N, 151°17.68'W	5197	BC,THIEL
DOMES #1	DJ29	11/29/1977	9°23.37'N, 151°15.58'W	5183	BC,THIEL
DOMES #1	DJ30	11/30/1977	9°25.32'N, 151°9.95'W	5175	BC,THIEL
DOMES #1	DJ31	11/30/1977	9°29.5'N, 151°0.6'W	5199	BC,THIEL
DOMES #1	DJ32	11/30/1977	9°16'N, 151°56.1'W	5043	BC,THIEL
DOMES #1	DJ34	12/1/1977	9°16.7'N, 151°9.8'W	4842	BC,THIEL
DOMES #1	DJ35	12/2/1977	9°19.34'N, 151°28.92'W	5130	BC,SANDIA
DOMES #1	DJ36	12/2/1977	9°26.65'N, 151°32.84'W	5231	BC,SANDIA
DOMES #1	DJ37	12/2/1977	9°25.5'N, 151°38.3'W	5197	BC,SANDIA
DOMES #1	DJ38	12/3/1977	9°36.3'N, 151°58'W	5086	BC,SANDIA
DOMES #1	DJ39	12/3/1977	9°35.8'N, 151°6.8'W	5117	BC,SANDIA
DOMES #2	DJ40	5/18/1978	9°23.5'N, 151°29.2'W	5256	BC,SANDIA
DOMES #2	DJ41	5/18/1978	9°22.7'N, 151°28'W	5191	BC,SANDIA
DOMES #2	DJ42	5/19/1978	9°23.6'N, 151°28.1'W	5219	BC,SANDIA
DOMES #2	DJ44	5/19/1978	9°24.5'N, 151°27.5'W	5235	BC,SANDIA
DOMES #2	DJ46	5/19/1978	9°28'N, 151°27.6'W	5216	BC,SANDIA
DOMES #2	DJ47	5/20/1978	9°21'N, 151°28.7'W	5208	BC,SANDIA
DOMES #2	DJ48	5/20/1978	9°22'N, 151°25.9'W	5165	BC,SANDIA
DOMES #2	DJ49	5/20/1978	9°23.4'N, 151°25.3'W	5171	BC,SANDIA
DOMES #2	DJ50	5/20/1978	9°22.1'N, 151°24.6'W	5086	BC,SANDIA
DOMES #2	DJ52	5/21/1978	9°18.4'N, 151°26'W	5093	BC,SANDIA
DOMES #2	DJ54	5/22/1978	9°20.7'N, 151°24.5'W	5064	BC,SANDIA
DOMES #2	DJ55	5/22/1978	9°27'N, 151°34'W	5246	BC,SANDIA
DOMES #2	DJ56	5/22/1978	9°20.1'N, 151°30.1'W	5159	BC,SANDIA
DOMES #2	DJ58	5/23/1978	9°20.2'N, 151°33.1'W	5148	BC,SANDIA
DOMES #2	DJ59	5/23/1978	9°17.6'N, 151°33.3'W	5011	BC,SANDIA
DOMES #2	DJ60	5/23/1978	9°20'N, 151°26.2'W	5196	BC,SANDIA
DOMES #2	DJ62	5/24/1978	9°15.2'N, 151°16.5'W	4921	BC,SANDIA
DOMES #2	DJ63	5/24/1978	9°24.8'N, 151°30.2'W	5215	BC,SANDIA
DOMES #2	DJ65	5/25/1978	9°26.4'N, 151°32.2'W	5253	BC,SANDIA
DOMES #2	DJ66	5/25/1978	9°27'N, 151°35.9'W	5250	BC,SANDIA
DOMES #2	DJ69	5/25/1978	9°15.8'N, 151°30.7'W	5049	BC,SANDIA

Table 1 (continued)

PROGRAM	Sample	Date	POSITION	Depth (m)	Sampler
DOMES #2	DJ70	5/26/1978	9°16.7'N, 151°28.7'W	4942	BC,SANDIA
DOMES #2	DJ72	5/27/1978	9°33.8'N, 151°21.3'W	5240	BC,SANDIA
DOMES #2	DJ73	5/27/1978	9°28.1'N, 151°15.6'W	5107	BC,SANDIA
DOMES #2	DJ74	5/27/1978	9°24.4'N, 151°17.9'W	5283	BC,SANDIA
DOMES #2	DJ75	5/27/1978	9°23.7'N, 151°17.1'W	5216	BC,SANDIA
DOMES #2	DJ77	5/28/1978	9°21.3'N, 151°20.5'W	5034	BC,SANDIA
ECHO I (C)	H347	6/13/1983	14°38.28'N, 125°26.99'W	4511	BC,SANDIA
ECHO I (C)	H348	6/13/1983	14°38.07'N, 125°27.65'W	4504	BC,SANDIA
ECHO I (C)	H349	6/14/1983	14°38.39'N, 125°27.18'W	4517	BC,SANDIA
ECHO I (C)	H350	6/14/1983	14°38.12'N, 125°26.82'W	4506	BC,SANDIA
ECHO I (C)	H351	6/14/1983	14°37.63'N, 125°26.38'W	4516	BC,SANDIA
ECHO I (C)	H352	6/14/1983	14°38.21'N, 125°26.32'W	4502	BC,SANDIA
ECHO I (C)	H360	6/17/1983	14°41.38'N, 125°27.53'W	4500	BC,SANDIA
ECHO I (C)	H362	6/18/1983	14°42.08'N, 125°25.86'W	4480	BC,SANDIA
ECHO I (G)	H359	6/18/1983	14°41.13'N, 125°23.01'W	4566	BC,SANDIA
ECHO I (N)	H361	6/18/1983	14°40.8'N, 125°22.04'W	4567	BC,SANDIA
ECHO I (T)	H353	6/18/1983	14°42.09'N, 125°24.27'W	4516	BC,SANDIA
ECHO I (T)	H354	6/18/1983	14°41.81'N, 125°24.22'W	4514	BC,SANDIA
ECHO I (T)	H355	6/19/1983	14°41.97'N, 125°24.27'W	4510	BC,SANDIA
ECHO I (T)	H356	6/21/1983	14°42.45'N, 125°24.27'W	4518	BC,SANDIA
ECHO I (T)	H357	6/23/1983	14°42.14'N, 125°24.28'W	4510	BC,SANDIA
ECHO I (T)	H358	6/23/1983	14°42.19'N, 125°24.26'W	4516	BC,SANDIA
BPRA 1	PRA02	10/04/1989	12°56.06'N, 128°21.94'W	4815	BC,SANDIA
BPRA 1	PRA04	10/04/1989	12°55.48'N, 128°19.6'W	4708	BC,SANDIA
BPRA 1	PRA05	10/04/1989	12°56.81'N, 128°20.66'W	4741	BC,SANDIA
BPRA 1	PRA06	10/04/1989	12°55.27'N, 128°21.53'W	4833	BC,SANDIA
BPRA 1	PRA08	10/05/1989	12°54.57'N, 128°20.7'W	4797	BC,SANDIA
BPRA 1	PRA12	10/06/1989	12°56.91'N, 128°18.91'W	4828	BC,SANDIA
BPRA 1	PRA13	10/06/1989	12°55.07'N, 128°16.96'W	4775	BC,SANDIA
BPRA 1	PRA14	10/06/1989	12°58.12'N, 128°19.63'W	4809	BC,SANDIA
BPRA 1	PRA15	10/06/1989	12°55.5'N, 128°19.23'W	4741	BC,SANDIA
BPRA 1	PRA16	10/07/1989	12°55.84'N, 128°18.9'W	4848	BC,SANDIA
BPRA 1	PRA17	10/07/1989	12°58.31'N, 128°21.96'W	4854	BC,SANDIA
BPRA 1	PRA18	10/07/1989	12°58.64'N, 128°17.84'W	4835	BC,SANDIA
BPRA 1	PRA19	10/07/1989	12°58.31'N, 128°20.8'W	4746	BC,SANDIA
BPRA 1	PRA20	10/07/1989	12°58.44'N, 128°21'W	4794	BC,SANDIA
BPRA 1	PRA21	10/08/1989	12°58.64'N, 128°19'W	4782	BC,SANDIA
BPRA 1	PRA22	10/08/1989	12°57.92'N, 128°17.75'W	4797	BC,SANDIA

Programs *DOMES #1* and *DOMES #2* are samples taken at DOMES site A on 1977 and 1978 (Jumars 1980). Program *ECHO I* indicates samples taken at DOMES site C on 1983 (Spiess et al. 1984). Program *BPRA1* indicates samples taken at the PRA site (Wilson 1990a, 1992). *ECHO I* sample types: (C) control sample, (G) geology only sample, (N) sample with no nodules, and (T) test sample placed near the miner track

fauna for which most life stages were retained on a 0.3-mm mesh screen. Megafauna (animals that might be visible in photographs) were rare in the samples, so this size class is not evaluated here. Meiofauna (taxa for which many life stages and species would pass through a 0.3 mm screen), although enumerated in the programs, are also not considered.

DOMES site A

Box corer samples were taken in a 35-km by 60-km area (Fig. 2): 24 biology samples were collected in November 1977; 26 biology samples were taken in May 1978. The sample locations were selected by picking points at random from

an inner 10-km by 30-km area and from the remaining area separately. Sample locations were determined within a transponder net operated by Ocean Management Incorporated (cruise 1) or using ranges to a radar buoy at the site with an average positional accuracy of approximately ~0.5 km (cruise 2). Piper and Blueford (1982) provide a chart of the sample locations, although not all samples were used for biological purposes. Mining was not carried out in the previously agreed impact site, so samples during the second biological cruise were not taken directly in the impacted areas (Jumars 1980). Because before (1977) and after (1978) mining samples did not appear significantly different (Jumars 1980), both datasets are treated as representative of the background benthic community. The NOAA R/V *Oceanographer* cruises to Site A in 1977–1978 used two versions of the USNEL 0.25-m² box corer. One corresponded to that described by Hessler and Jumars (1974; see also Thiel 1983) except that the vent doors were on the top of the coring head rather than on the sides (design by H. Thiel). This device was used to collect box cores numbered DJ08 through DJ34. The remaining samples were collected with a box corer modified according to designs prepared by R. R. Hessler, P. A. Jumars, and J. Finger (sometimes referred to as the “Sandia” box corer). A comparison of isopod crustacean fractions collected by the two corers revealed no apparent difference in their sampling efficiency (Jumars 1980). The corer box on either sampler contained no in situ subcores. On recovery, the top water was drained through a 0.3-mm mesh sieve and the screen residues were added to the main biological sample. A subcore with an internal area of 46 cm² was taken for geological analysis (data in Piper and Blueford 1982). The macrofaunal samples thus represent a surface area of 2454 cm². The nodules were washed and inspected for visible macrofauna; screen residues from the nodule wash were saved as a separate fraction. Nodules were then taken for geological analysis (Piper and Blueford 1982). The top 1 cm was washed gently on a 0.3-mm mesh sieve. A 9-cm-deeper layer was placed in an elutriation device (Hessler and Jumars 1974) and washed through the same size sieve. The screen residues were fixed in a sodium borate-buffered formaldehyde in filtered seawater (1:5 by volume; sodium borate is no longer recommended as a buffer because it macerates specimens left for long periods), and then later preserved in 80% ethanol after a freshwater rinse. In the laboratory of P. A. Jumars at the University of Washington, macrofaunal taxa were sorted under a dissecting microscope. Not all lower 9-cm layers were completely sorted, so only 41 samples were for density calculations.

DOMES site C

During the Echo I cruise, the modified “Sandia” 0.25-m² box corer with improved box and vent door seals (Wilson and Hessler 1987) was used to collect quantitative samples

(Table 1; Fig. 3). For macrofaunal processing, each sample was divided into 6 separate fractions: top water, nodule washings, aspirator water (material sucked up from surface puddles of fluid and sediment), 0–1 cm layer, 1–5 cm layer, and 5–10 cm layer. This layering facilitated rapid fixation of the animals and permitted an approximate analysis of the depth distribution of the fauna. Most animals were in the fractions with the least sediment, thereby avoiding mechanical damage to the specimens and facilitating their rapid removal from the sediment during sorting. All nodules were washed and examined to remove large encrusting fauna. Some nodules were preserved for a study of the epifauna (see Mullineaux 1987, 1988a, b, 1989). The sedimentary fractions were sieved with 0.3-mm screens during the cruise. The entire top 1 cm layer and the screen residues of the lower layers were directly placed in 4% buffered formaldehyde-seawater for fixation. The larger volume fractions (1–5 cm layer, and 5–10 cm layer) were washed through a 0.3-mm screen using an elutriation device. After several days of occasional gentle agitation to aid fixation, the screen residues were washed with freshwater and placed in 80% ethanol for long-term preservation. The samples were sorted to major taxa using Wild M5 stereomicroscopes in the laboratory of R. R. Hessler at the Scripps Institution of Oceanography. Another cruise, “Quagmire II”, to site C (Wilson 1990c) the same locality as the ECHO I cruise, is not considered here.

PRA site

The box corer used at the PRA site (Table 1; Figs. 4, 5) was the same as that used at DOMES site C. All samples were divided on recovery of each sample into approximate vertical layers: top water, aspirator water, nodules and nodule wash, top 1 cm, 1–5 cm, and 5–10 cm. These layers, although not truly quantitative, provided a qualitative indication of the depth distribution of the fauna. Consequently, this layering was maintained in the laboratory and all fractions were sorted separately. Initial fixation of all fractions on the R/V *Moana Wave* used 4% buffered formaldehyde-seawater; after 4–6 days, the samples were washed and transferred to alcohol. Each fraction was washed with 25% ethanol in 0.3-mm mesh screens and then immersed in rose bengal for a short period (often overnight) to stain the protein-rich particles, usually specimens that were alive at sampling. In the laboratory, the major taxa were sorted into vials containing 80% ethanol and counted. The contents of selected vials were examined a second time to verify identifications. All animals were removed from the samples, including the Foraminifera. In some cases, individuals could not be counted because the group was colonial (Bryozoa, Hydrozoa, Porifera) or were highly fragmented and not possible to identify specific

individuals (Foraminifera). Their presence was indicated by a nominal 1 individual in the relevant layer.

Species identification

Data for species-level identifications are available for polychaetes, isopods and tanaids at all sites ([supplementary material](#)). Morphospecies were identified for tanaids for DOMES sites A and C (ECHO I). Isopoda and Polychaeta were identified by taxonomic experts and coordinated across all sites, whereas non-isopod Peracarida and other macrofauna were identified to morphospecies at the site C. Polychaeta were identified by the late Kristian Fauchald at site A and by Kirk Fitzhugh at site C and the PRA site, who coordinated his identifications with the site A identifications. The taxonomic nomenclature in the data tables has not been updated since 1987. I identified all isopod species, with partial illustrations; most taxonomy in the data tables has been updated. Tanaids morphospecies were identified for DOMES sites A and C by Timothy Ragen and myself with consultation from the late Jurgen Sieg. Literature on most tanaid genera was collected to assist placing specimens into relevant genera; the data tables have not been updated from 1987. In a few cases, the number of taxonomically reported individuals may differ from the total for that taxon in the sorting results summaries. These numbers have not been changed to avoid ad hoc decisions on which observation was correct. All species diversity analyses omitted specimens not identified to species.

Specimen deposition

All material treated in this manuscript from all three sites, as well as meiofauna and other taxa except for the molluscs and the samples from the Quagmire II cruise, were transferred in the United States Museum of Natural History, Smithsonian Institution, collections. The Mollusca were deposited in the Malacology Collection at the Australian Museum.

Production estimates

Chih-Lin Wei (personal communication; Sweetman et al., in preparation) provided estimates for the CCFZ sites for average monthly chlorophyll-a (CHL) for years 1998–2014, net primary productivity (NPP) was estimate using the Monthly Vertical General Production Models (VGPM) from www.science.oregonstate.edu/ocean.productivity. Export particulate organic carbon (POC) flux is based on the Lutz et al. (2007) algorithm, which used a long-term monthly average of NPP (1998–2014) by multiplying an export ratio that is directly related to seasonality. The samples were collected during the decades earlier than the time range of the productivity data and therefore not representative of productivity conditions during the time of the sampling owing to decadal shifts in productivity (Smith et al. 2013). This being the case, the values are considered to be indicative of

the relative productivity differences between the three sites. Thus, we expect that the most western site will have substantially lower productivity values than the two eastern sites.

Species diversity assessment

The data for each taxon (Polychaeta, Isopoda, Tanaidacea) were trimmed of specimens not identified to species. Most analyses and plots were done in LibreOffice Calc. Hypergeometric model means, i.e., Sanders rarefaction plots (Sanders 1968; Hurlbert 1971), were calculated using my Pascal program EXPSPP, based on a Fortran program written by P. A. Jumars. The rarefactions were compared to results from other biodiversity programs, BioDiversity Pro v.2 (BDPRO; McAlecece et al. 1997) and EstimateS (Colwell 2013); all programs consistently reported the similar values within 0.25% ([supplementary material](#)). The bootstrapped lognormal distribution calculations were calculated using my Pascal program BOOTLOGN (current v. Bootln2016, based on a Fortran algorithm written by G. Sugihara (1980) using the doubly truncated lognormal distribution (Cohen 1950), log base 2. The lognormal distribution has been thought to be problematic because it is not based on a statistical sampling model (e.g., Colwell and Coddington 1994; Chao and Chiu 2016). This has been addressed by a nonparametric bootstrap estimator (Efron 1979; Efron and Gong 1983) that creates many pseudoreplicates (with replacement) of the original data to provide mean total species, along with variance and confidence limits. A fuller explanation of the methods can be found in Wilson (1987a; [supplementary material](#)). Bootstrap estimates were based on 1000 pseudoreplicate samples of the original species abundance data. The CHAO1 estimator (Chao 1984; Colwell and Coddington 1994) in EstimateS and BDPRO was tried on the polychaete data ([supplementary material](#)); CHAO1 found the approximate lower bound of the bootstrapped results, suggesting that nonrandom clumped distributions were impacting the frequency of singletons and doubletons, on which the index depends. The lognormal estimator uses the species abundance values directly, so should be less affected by contagious distributions. Ordinations were conducted on the species-level data but are not reported because the sparse matrices did not provide strong results.

Faunal similarity

Normalized expected species shared (NESS; Grassle and Smith 1976) was used to assess faunal similarity for each of the taxa. Original implementations of this method gave anomalously high values (>1.0) in matrices like the isopod and tanaid datasets where many species are present as only single individuals. A revised version of the NESS algorithm (NEWNESS, E. Gallagher, personal communication) was used as a program compiled in Fortran77. Similarities are reported either at a shared

species of $m = 50$ for comparability or using m_{\max} , the maximum number of shared species for the set of samples so that the index is sensitive to rare species.

Data repository

Faunal data and an extended discussion of the bootstrapped lognormal estimator are available in the [supplementary material](#). Additional data and detailed analyses, as well as Linux binaries of Bootlogn and ExpSpp, are available from me on request.

Results

Faunal assessment, DOMES site A

The faunal data for DOMES site A study is from Jumars (1980), although other reports covered portions of the fauna (Glover et al. 2002; Paterson et al. 1998; Thistle and Wilson 1987, 1996; Wilson 1987a, b). Jumars (1980), however, only discussed the statistical outcome relative to the before and after OMA test mining impact, so the data in that report are the main source of information (Tables 2, 3). Only 41 of the 52 macrofauna samples were completely sorted, so only the complete data were used for the summary values. All samples, however, contributed to the species data (see “[Species diversity and turnover between CCFZ sites](#)”). The most abundant group in the fauna was Polychaeta (38.57%) followed by Tanaidacea (12.83%) and Isopoda (11.91%). The sessile groups associated with nodules (Porifera, Tunicata, Entoprocta and Bryozoa) together made a substantial fraction (14.69%) of the total fauna. The samples were not fractioned to the level used in latter programs, although data from nodules and top 1 cm were kept separated in many samples. Where the nodule and top fractions were kept separate, they accounted for an average of 68.1% of the fauna in each sample, with 15.6% from the nodules and 56.4% from the top layer. Macrofauna abundances were poorly correlated with either nodule abundances ($R^2 = 0.19$) or depth ($R^2 = 0.03$) at this site. Jumars (1980) found substantial spatial autocorrelation in the DOMES site A samples, so that adjacent samples closely resembled one another.

Faunal assessment, DOMES site C – ECHO I locality

Samples at this site were grouped as potential mining impact samples being near mining tracks (“tests”) or those taken away from the mining tracks (“controls”). All samples except one (H361) had manganese nodules. Macrofauna numbers varied considerably (43 individuals, H352 to 155 individuals, H349; Table 4) in the 15 samples (Fig. 3). The average density of macrofauna was 370.7 ind/m^2 [standard deviation (SD)

123.92]. The test samples had a higher mean abundance than the controls, 96 versus 82.6 individuals, but the tests were less variable, test (SD = 16.6) compared to the controls (SD = 32.8), because the test sample area was clustered around miner tracks and therefore were from a smaller area. Similar to DOMES site A, most of the fauna lives at the surface. In all, the top 1 cm layer, nodule wash and other filtered water from the surface (aspirator water, top water) accounted for 71.12% of the fauna the samples. The lower two layers (1–5 cm, 5–10 cm) accounted for 21.41 and 7.47% of the fauna, respectively. A substantial number of individuals appeared in the nodule wash (15.80% of the total), demonstrating that many taxa were living on the nodules. These include Brachiopods, some Ascidacea, some Cnidaria, limpet-like Gastropoda, Monoplacophora, Polyplacophora, Porifera, and some Polychaeta. These groups either fell off the nodules during sampling or they were removed during the washing procedure. A few specimens proved to be highly tenacious, and remained on the nodules that were preserved for later study (L. Mullineaux, personal communication); because those specimens were so few, their omission from the results reported here should not greatly affect our conclusions. As expected, the Polychaeta were the most abundant group, with the greatest numbers in control sample H349, and “no nodule” sample H361 (Table 4). The arthropods were the second most abundant group in these samples, being dominated by the Tanaidacea and the Isopoda. The Mollusca were the third most abundant group, within which the gastropods and the bivalves were most abundant.

Faunal assessment, PRA site

The summary macrofaunal data are in Table 5. The average density of macrofauna is 774.50 ind/m^2 (SD 254.8) over a range of 444 (PRA18) to 1324 (PRA17) individuals. These densities are 2 times higher than those seen at the DOMES site C (ECHO I locality). Macrofaunal density was inversely correlated with depth; slope = -0.268 , although although weakly ($R^2 = 0.055$), mostly due to the influence of outlier PRA17. This inverse relationship is improved if PRA17 is removed from the data set (slope = -0.623 , $R^2 = 0.429$). Relationships with nodule densities or maximum sizes were not apparent probably because nodules have much less coverage at PRA than at other sites. Unlike the other sites, the PRA site shows a slightly deeper penetration into the sediment by the fauna. While the top layers (nodules, washes and top 1 cm) account for 62.51% of the fauna, 37.5% of the fauna were found below 1 cm (1–5 cm 27.97%; 5–10 cm, 9.52%). This might be attributed to the higher water content of the sediments.

Comparative faunal abundances

Of the three sites, PRA showed the highest abundances in all categories (Table 6) and DOMES site A had the least. Correlated with the east to west decrease in surface and sea

Table 2 DOMES site A, 1977 cruise macrofauna data

Taxon	DJ02	DJ08	DJ10	DJ11	DJ12	DJ13	DJ15	DJ16	DJ18	DJ20	DJ21	DJ23	DJ24	DJ25	DJ26	DJ28	DJ29	DJ30	DJ31	DJ32	DJ34	DJ35	DJ36	DJ38	DJ39
Porifera	3	6	2	4	7	7	2	3	13	8	4	8	8	2	2	2	2	1	7	6	6	11	11	14	
Cnidaria	1		2	1	2	1	1	2	1	1	1	1	3	1	2	2	2	1			3	2	2		
Nemertea							1																		
Polychaeta	26	36	11	11	7	14	14	15	9	13	24	9	21	23	14	28	23	21	7	19	35	20	17	34	20
Oligochaeta	1															1	2		2						
Sipunculida							1			1												2			
Echiura							1															1			
Cumacea																									
Tanaidacea	7	7	7	6	3	7	8	5	5	7	6	10	8	7	4	6	8	2	2	9	10	10	4	11	8
Amphipoda	1						6			2	1	1	1	1	1	1	1	1	3	1	1				
Isopoda	6	11	4	1	4	4	7		1	12	4	7	7	3	2	7	2	4	13	6	7	1	3	13	
Peracarida unident									4																
Decapoda										1															
Aplacophora										1						2			1		4		1		
Monoplacophora											1														1
Polyplocophora																									1
Bivalvia	3	4	7	1	2	7	2	5	3	6	4	5	1	4	10	2	12	1	4	4	4	7	4	6	1
Gastropoda	1	1	2	2	3	1	1	2	2	2	3	1	3	2	1	1	1	9	2	4	4	1	1	1	2
Scaphopoda	1									1					1				1						
Ophiuroidea																									1
Holothuroidea																									1
Crinoidea																									1
Echinoidea																									1
Priapulida																	2								1
Brachiopoda	1	1					1		2	2	5	1	5	1	1	1	1	1	1	1	1	2			2
Bryozoa solitary	11		32				12		11	1	6	1	1	1	4				100			15			3
Bryozoa colonies	1								1	6	1	1													
Entoprocta																									
Acidacea																									
solitary colonies																1			1						1
Enterpneusta																									
Insectae sedis	2	2	2	2	2	2	1	1	1	1	2	4	1	1	4	1	1	1	1	1	1	1	2		2
Total	58	70	37	61	19	50	33	53	28	74	60	38	59	46	28	69	43	54	12	163	68	54	66	59	61

Table 3 DOMES site A, 1978 cruise macrofauna data

Taxon	DJ 40	DJ 41	DJ 42	DJ 44	DJ 46	DJ 47	DJ 48	DJ 49	DJ 50	DJ 52	DJ 54	DJ 55	DJ 56	DJ 58	DJ 59	DJ 60	DJ 62	DJ 63	DJ 65	DJ 66	DJ 69	DJ 70	DJ 72	DJ 73	DJ 74	DJ 75	DJ 77	Total both cruises
Porifera	3	1		1	2	3	7	7	1	1	1	1	7	1	3	1	2	2	6	3	3	3	4	3	1			153
Cnidaria	2				2				2				1	1			1											36
Nemertea																					1							2
Polychaeta	31	21	24	33	23	28	4	36	13	23	28	12	32	41	18	28	22	17	13	28	15	22	17	20	12	17	33	1082
Oligochaeta	2			1	1		3	3		2	2	2	2	1	1					3	3							24
Sipunculida																				1				1				6
Echiura																												2
Cumacea				1																1								4
Tanaidacea	7	17	6	5	3	4	2	6	13	8	7	6	12	6	8	11	8	7	5	11	9	9	5	10	2	6	6	360
Amphipoda	1	4	1	1	1	2	2	2	2	1	1	1	1	1	1	1	3			1	1	1	1	2	1	1	1	43
Isopoda	11	12	4	3	11	5	2	3	10	12	4	2	8	8	8	5	8		5	3	14	28	11	13	1	7	7	334
Peracarida																												4
unidentified																												
Decapoda																		2		1		1						4
Aplacophora											2		1	2		1												19
Monoplacophora																												2
Polyplacophora																												2
Bivalvia	12	12	2	7	5	4	1	2	2	5	4	4	7	4	1	8	2	6	8	6	4	7	2	1	1	10	3	240
Gastropoda	1				9	3	2	2	3	1	1	3	1			1			2	2	2	1	1					78
Scaphopoda																												6
Ophiuroidea	1																	1										9
Holothuroidea																												4
Crinoidea																												1
Echinoidea				1																	1					1		4
Priapulida																												5
Brachiopoda	1			3		1		4	1	1		1			2					2	1	2						34
Bryozoa solitary	1	7	1	3	2	2	1	1	1											13		1	2					217
Bryozoa colonies																				4	1	2						20
Entoprocta	1					1	4	9		5	20						1			4	4	2						54
Acidacea solitary	1																			3		1						15
Acidacea colonies	1																											1
Enterpneusta																												1
Insertae sedis	1			4	3		1	1	1	1	1	1	1	1	1	4				1	1	1	1					39
Sample Total	72	76	42	62	58	55	17	74	46	59	68	33	72	65	42	65	46	36	39	60	75	74	43	49	18	39	57	2805

Table 4 DOMES site C (ECHO I), abundances of major macrofaunal taxa

Station	H347	H348	H349	H350	H351	H352	H353	H354	H355	H356	H357	H358	H360	H361	H362	Total
Taxon																
Annelida -																
Polychaeta	18	40	80	34	46	21	57	47	40	55	48	45	32	87	28	678
Siboglinidae	0	0	0	1	0	0	0	0	0	0	0	0	0	0	0	1
Sipunculida	0	0	1	1	0	1	0	0	0	0	0	0	0	0	0	3
Priapulida	1	0	0	0	0	0	0	0	1	0	0	1	0	0	1	4
Unidentified-Worms	4	0	7	14	0	1	2	0	0	0	0	1	1	3	0	33
Arthropoda -																
Amphipoda	0	2	0	0	1	2	0	6	0	2	1	4	2	0	0	20
Cumacea	0	2	0	0	1	0	0	1	0	1	0	0	0	1	0	6
Isopoda	8	4	30	6	6	2	12	11	5	15	23	7	5	11	8	154
Tanaidacea	11	21	17	10	10	9	6	16	8	13	14	15	11	13	9	183
Ascidacea	10	0	1	1	1	1	17	0	0	1	5	0	0	0	1	38
Brachiopoda	1	0	0	1	0	0	0	1	0	0	0	3	1	0	1	8
Bryozoa	5	5	6	3	1	2	0	5	8	3	5	3	0	10	2	58
Cnidaria	0	0	0	3	0	1	0	3	0	1	1	4	2	3	3	21
Echinodermata -																
Echinoidea	0	0	0	0	1	0	0	0	0	1	0	0	0	0	0	2
Holothuroidea	2	1	0	0	8	0	0	0	1	0	0	1	0	1	3	17
Ophiuroidea	1	1	2	0	0	0	0	0	0	2	4	0	1	0	0	11
Entoprocta	0	0	0	0	0	0	0	0	0	0	0	1	0	0	0	1
Mollusca -																
Solenogastres	0	2	0	0	0	0	1	0	0	1	1	1	0	1	2	9
Bivalvia	3	6	3	4	5	1	5	5	2	4	2	1	8	21	4	74
Archaeogastropoda	1	0	2	0	6	2	1	2	0	0	4	1	0	0	1	20
Other Gastropoda	2	2	4	1	2	0	0	2	0	1	2	2	3	2	3	26
Monoplacophora	0	0	0	0	1	0	0	3	0	0	0	0	0	0	0	4
Polyplacophora	0	1	1	1	1	0	0	0	0	0	0	0	0	0	0	4
Scaphopoda	0	1	1	0	0	0	0	1	0	0	0	0	2	0	0	5
Porifera	1	1	0	0	0	0	0	3	0	1	0	1	0	1	2	10
Total	68	89	155	80	90	43	102	106	65	101	111	91	68	153	68	1390

floor export production (Wei, personal communication), the mean faunal density (macrofaunal ind/m²) also decreased (Table 6). The PRA site had the highest values for CHL, NPP and POC as well as values for macrofaunal density. Although the CHL values for sites A and C (showing the best linear correlation with macrofauna density: $R^2 = 0.9896$) are minimally lower than the PRA site (70.25 and 80.89%, respectively), the macrofaunal abundances and all components of the fauna are substantially much higher at PRA than at sites A and C (29.04 and 47.86% of PRA abundances, respectively). Data for peracarids and polychaetes are provided in Table 6 but these differences are parallel across all members of the fauna. This great disparity between the mean productivity and the macrofaunal abundances (Table 6) may be the result of the persistence of deep-sea populations, thus integrating POC flux at the sea

floor over a longer time frame than the available measurements (1998–2014). Another possibility might be the PRA site experienced especially high productivity during the decade 1980–1989 than was observed during the 1998 to 2014 time frame of the productivity estimates. Subjective observations in 1989 indicated that region around the PRA sites had high fish populations; fishing ships were seen all around the R/V *Moana Wave* while on station.

Species diversity and turnover between CCFZ sites

Summary data are presented in Tables 7, 8 and 9, and the full data can be found the [supplementary material](#) archived with this journal. The taxocenes Polychaeta, Isopoda and Tanaidacea are treated separately owing to differences in presumptive dispersal characteristics and population dynamics.

Table 5 PRA site, abundances of major macrofaunal taxa

Sample	02	04	05	06	08	12	13	14	15	16	17	18	19	20	21	22	Total
Mollusca																	
Aplacophora		1	1		1	1	1	1	1	1		1	1		2	1	13
Gastropoda	2	4	4		1			2	9	2			5		2	4	35
Scaphopoda	10	3		1	1		5	6	1	3	3	3	4		2	1	43
Bivalvia	4	7	9	7	8	1	11	7	5	8	124	5	3	9	7	2	217
Annelida																	
Polychaeta	85	80	51	69	90	58	72	55	80	88	135	45	186	54	97	111	1356
Oligochaeta	3	4	3	5	3		5	5	6	5	2		9	2	2	4	58
Peracarida																	
Cumacea	1	2			1		2	1	1				1		1	4	14
Tanaidacea	19	30	22	10	11	7	20	15	40	27	14	15	35	32	32	45	374
Isopoda	17	30	6	16	20	17	26	26	23	16	28	21	34	14	14	21	329
Amphipoda	2	3	2	2	1	2		3		2	2	1	4		4	1	29
Decapoda	1																1
Porifera	3	6	12	2	10	14	5	2	5		2	1	2	1	1	2	68
Coelenterata																	
Hydrozoa	16	15	24	6	12	6	5	4	6	1	1		3			1	100
Anthozoa			2					1	1		1						5
Turbellaria					1												2
Nemertea	4	13	11	8	20	10	14	11	6	6	6	6	28	11	23	38	215
Priapulida							1										1
Sipunculida	2	2	4			1	1			1		2	3	3		1	20
Echiura										1						1	2
Bryozoa	4		3		1			1	3		8	5		2	4	1	32
Brachiopoda			1														1
Entoprocta	11	1		3		1		2	3						5	6	32
Echinodermata																	
Ophiuroidea		1	2			1		1	4			1	1				11
Echinoidea	4	1			2						1	1					9
Holothuroidea			2					1	1			2			1		7
Crinoidea	1	2	10			1			3				3				20
Asteroidea														1			1
Hemichordata																	
Asciacea	1				1		2	3	2		2				1		12
Unidentified		7	16	2	2	12	2	7	4	1	2	2	4	7	2	1	73
Total	197	213	185	131	189	134	173	154	204	164	331	111	329	137	201	245	3098

Polychaeta

Being the most abundant category of the fauna, both in individuals and in species (Table 7), places the polychaetes as the dominant member of the abyssal soft bottom assemblage. They might function as a proxy for rest of the fauna although other taxa should be considered independently. The reproductive mode of polychaetes possibly allows for long-range dispersal, although available evidence for abyssal regions indicates brooding behavior is frequent (Young 2003). Other reproductive modes seen in shallow water taxa, including

asexual budding and parthenogenesis, may also occur (e.g., spioniform families; Blake and Arnofsky 1999; Franke 1999). No consistent trends appear in the polychaete species diversity values. Although the PRA site had the greatest number of individuals and highest density, this site had the fewest species in the pooled samples. DOMES site C had the most species, but at an intermediate density. All rarefaction graphs have not reached an asymptote indicating that the total species count has not been recovered in the samples. These plots (Fig. 6) also do not cross, and are showing the same trends but at differing levels. The lognormal estimates of total

Table 6 Comparative macrofaunal abundances as mean individuals per square meter (ind/m²) from 0.25-m² box corer samples of 3 sites in the CCFZ, with production estimates

Site	DOMES site A	DOMES site C	PRA
Latitude (mean)	9°23.7'N	14°40.4'N	12°57'N
Longitude (mean)	151°26.9'W	126°25.3'W	128°19.8'W
Depth (mean)	5147	4500	4794
CHL	0.1018	0.1172	0.1449
NPP	264.64	321.55	359.15
POC	1.32	1.71	1.90
N (0.25 m ² box cores)	41	14	16
Macrofauna (mean ind/m ²)	224.88	370.67	774.50
Macrofauna (SD ind/m ²)	93.07	123.92	254.80
Selected taxa (ind/m ²)	(ind/m ²)	(ind/m ²)	(ind/m ²)
Polychaeta	83.61	187.73	339.00
Crustacea Peracarida	60.20	97.33	186.50
Isopoda	27.02	41.07	82.25
Tanaidacea	29.27	48.80	93.50
Amphipoda	3.32	5.33	7.25
Cumacea	0.20	1.60	3.50

CHL mean monthly chlorophyll A concentrations in mg/m²/month between 1998 and 2014 calculated using Morel and Berthon's (1989) Case I model, *NPP* monthly mean net primary production in mg C/m²/day over the same period using the monthly Vertical General Production Models (VGPM) from www.science.oregonstate.edu/ocean.productivity, *POC* mean export of particulate organic carbon to the sea floor in mg C/m²/day calculated using the Lutz et al. (2007) algorithm that employs the mean and seasonality (standard deviation/mean) of surface primary production, as well as the export depth below the euphotic layer

polychaete species (observed species and unobserved species, those below Preston's (1962a, b) veil line show a pattern that trends with density at each site (Table 7). Site A has the fewest estimated total species, while the PRA site is estimated to be the most species rich. The match of the lognormal distribution mode to the data was best for site A, but poorest for site C although substantially better than those found for the lower density crustacean taxa. The mode of the estimated lognormal

distribution (supplementary data) matched the sample distribution for site A, as indicated by the fit probability, but the sample mode was separated from the estimated mode by one standard deviation for site C and the PRA site. At all stations, the sample mode, the rarest species that were present as only singletons or doubletons, was the most common category, which leaves open the possibility that the distribution may change with additional sampling. The PRA

Table 7 Polychaeta species diversity indices

Site	DOMES site A	DOMES site C	PRA site
Species in sample (pooled)	105	115	97
Individuals in sample	774	636	1039
Density (mean ind/m ²)	83.61	187.73	339.00
Sample entropy (H')	3.8768	3.8661	3.5184
Sample evenness (J')	0.833	0.8148	0.7691
Expected spp at 100 ind	43.7	45.7	35.8
Expected spp at 500 ind	89.8	104.4	73.1
Lognormal estimated species	198.5	278.2	353.0
Chi-square fit	0.9338	3.0176	2.5557
Chi-square fit probability	0.9197	0.5549	0.7681
Bootstrap estimated species	202.9	274.1	310.1
Upper bound	206.2	280.3	317.6
95% confidence limits, t distribution			
Lower bound	199.6	267.9	302.6

See [Materials and Methods](#) for explanation

Table 8 Isopoda species diversity indices

Site	DOMES site A	DOMES site C	PRA site
Species in sample (pooled)	86	59	59
Individuals in sample	340	153	328
Density (mean ind/m ²)	27.02	41.07	82.25
Sample entropy (H')	3.9624	3.8343	3.5638
Sample evenness (J')	0.8896	0.9403	0.8740
Expected spp at 100 ind	48.9	49.4	38.2
Lognormal estimated total species	128.8	67.7	80.6
Chi-square fit	0.4253	0.6104	0.3721
Chi-square fit probability	0.8085	0.4346	0.8302
Bootstrap estimated total species	143.4	79.0	90.6
Upper bound	145.7	79.9	92.0
95% confidence limits, t distribution			
Lower bound	141.2	78.1	89.3

See [Materials and Methods](#) for explanation

site has the lowest evenness; this assemblage has a higher dominance (some species are much more common than others) and the tail of the lognormal distribution, the rare species, is longer, thus resulting a higher estimated total species. The bootstrapped lognormal estimates are preferred for site C and the PRA site because the fit of the original distribution was poorer, and because they are more conservative.

Considering the three sites in aggregate, a species accumulation plot (Figs. 7 and 8), similar to that done by Grassle and Maciolek (1992) based on individuals sampled and sample area sorted by longitude east to west, shows an almost perfect fit ($R^2 = 0.995$) to a logarithmic equation. A species accumulation plot based on individuals sampled is also modeled well by a logarithmic equation although not as closely ($R^2 = 0.968$). If the samples are sorted from west to east, however, linear equations fit the data better, probably because the

abundances were substantially lower in the site A samples. These regression models imply that polychaetes diversity will continue to increase as one takes more samples from the sites in aggregate. These equations do not, however, take account for unsampled areas between the sites, so assessing the similarity of the intermediate sites is needed for understanding beta diversity in the CCFZ (McClain and Rex 2015).

Isopoda

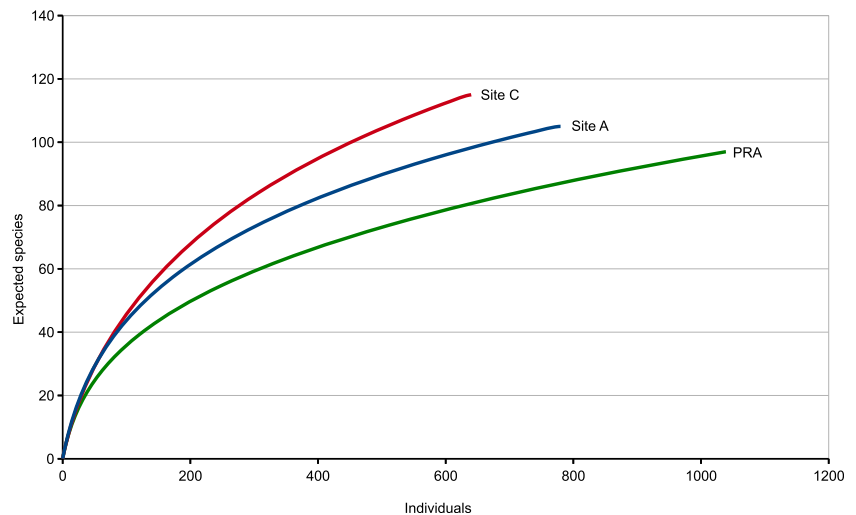
The peracarid crustaceans, and especially the Isopoda, are good representatives for that part of the fauna that has low dispersal potential. Asellota, which have no swimming larval dispersal phase in their life cycle (Wilson 1991), are the dominant isopod group in abyssal samples. Although some taxa may have presumptively higher dispersal potential as adults,

Table 9 Tanaidacea species diversity indices

Site	DOMES site A	DOMES site C
Species in sample (pooled)	61	46
Individuals in sample	354	172
Density (mean ind/m ²)	29.27	48.80
Sample entropy (H')	3.5903	3.3245
Sample evenness (J')	0.8734	0.8683
Expected spp at 100 ind	38.1	35.8
Lognormal estimated total species	81.8	100.6
Chi-square fit	2.8453	1.0443
Chi-square fit probability	0.4161	0.5932
Bootstrap estimated total species	85.6	112.0
Upper bound	86.5	115.7
95% confidence limits, t distribution		
Lower bound	84.8	108.3

See [Materials and Methods](#) for explanation

Fig. 6 Polychaeta. Sanders–Hurlbert rarefaction graph for DOMES site A, site C, and the PRA site



such as the Munnopsidae (Wilson 1989; Hessler 1993; Osborn 2009), most species are primarily non-natatory epifaunal or infaunal (Thistle and Wilson 1987, 1996). Descendant individuals of any isopod taxon, or any benthic animal in general, could potentially walk from one end of the CCFZ to the other, but then the question becomes at what distance can the taxon maintain gene flow. A isopod species probably cannot maintain genetic connectivity over this distance, given the patchy nature of the habitat and clumped dispersion pattern observed in deep-sea species (Jumars 1976).

The Isopoda have a distinctly different pattern of species diversity than found in the Polychaeta (Table 8) as well as much lower abundances. While polychaete species diversity showed a positive relationship with density and number of individuals, the isopods showed a negative relationship. Even though the PRA site has approximately the same number

of specimens as DOMES site A, it has 27 fewer species, a pattern that is also found in the total species estimates. Site C (ECHO I site) has the same number of species as the PRA site but many fewer individuals; the PRA isopod density (mean ind/m²) is twice that of site C. Additionally, site C has a rarefaction plot (Fig. 9) that rises quickly but crosses the site A graph to lower values at around 110 individuals. As in the polychaetes, the isopod collector's curves by individuals (Fig. 10) or by area (Fig. 11) are rising, so more species remain to be found, which is also supported by the log-normal fit to the isopod species abundance distributions (Table 8). Because the number of specimens included in the isopod data set were many fewer than the polychaetes, the fit of the data to lognormal distributions was poorer, to the extent that the site C data generated several “data set too small” warnings during bootstrap iterations. Half of the singletons

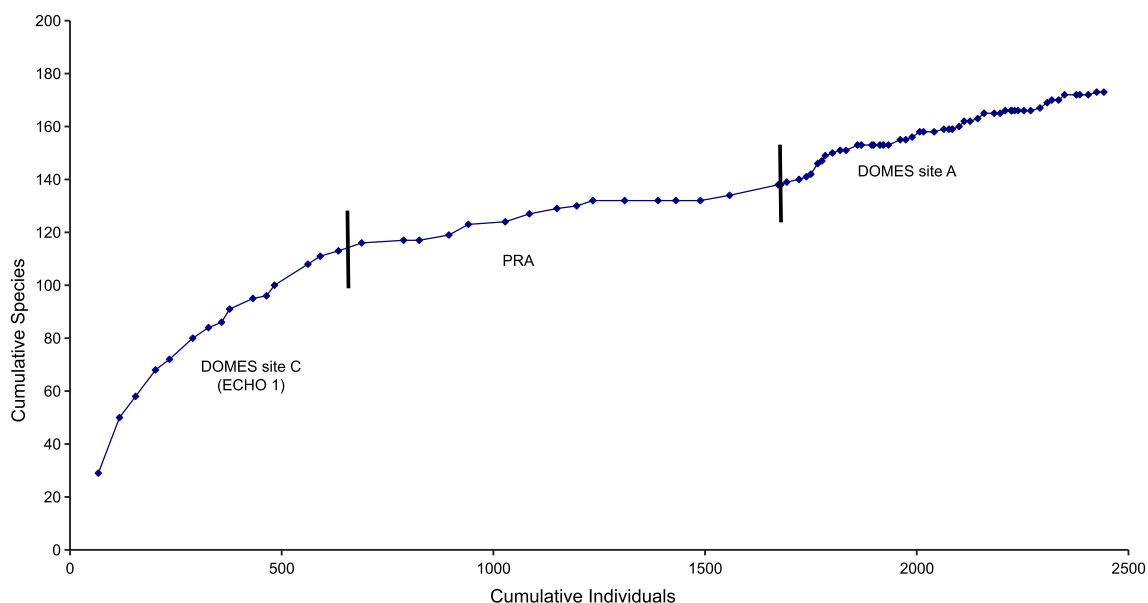


Fig. 7 Polychaeta. Species accumulated by individuals, oriented longitudinally east to west

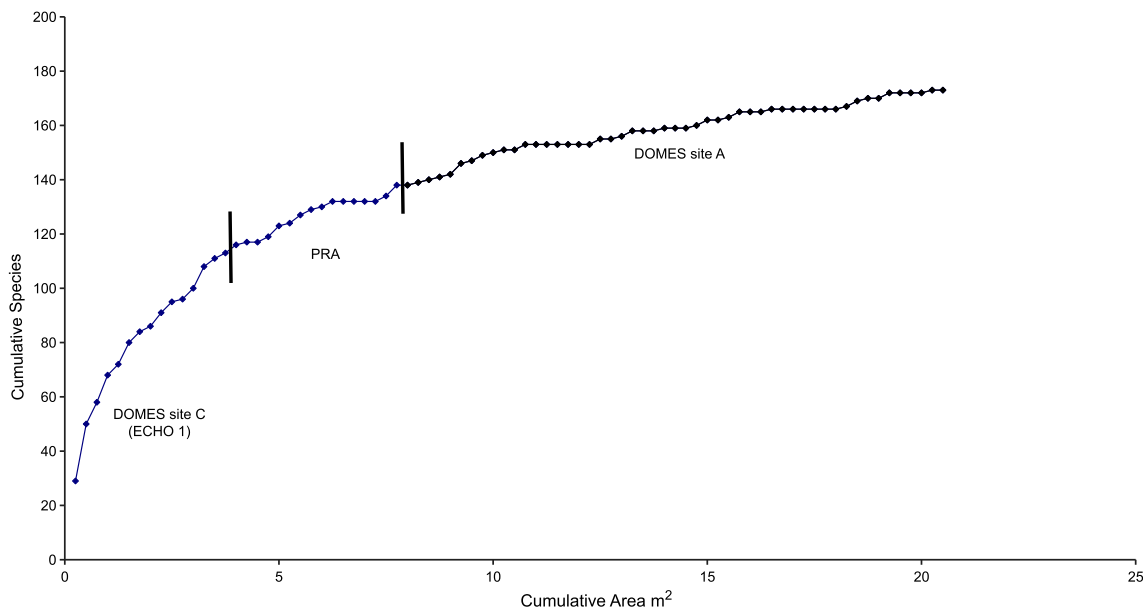


Fig. 8 Polychaeta. Species accumulated by area of samples, oriented longitudinally East to West

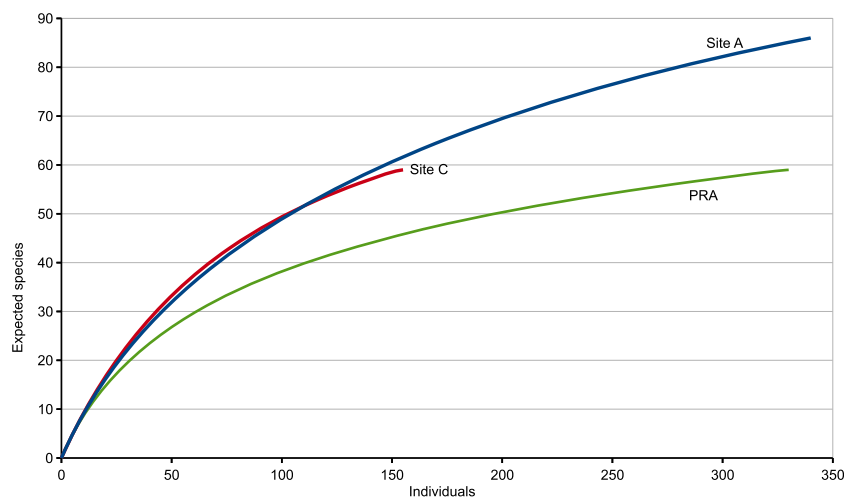
are not included in sample distributions so this most abundant category is especially reduced in the already small site C isopod dataset. In low abundance datasets such as these, poor lognormal estimates may result. The site A dataset, however, had an acceptable fit probability. The mode of the sample distributions were all within 1 standard deviation of the estimated distribution, although the patterns were substantially attenuated. The theoretical total species estimates follow the observed species in the samples, with site A having 143.7 species, PRA next with 90.6 and then site C with 79. The site C result is low owing to the small size of the data set.

Tanaidacea

The tanaids were identified to morphospecies for sites A and C; the PRA site specimens are currently unidentified. The tanaids represent a different reproductive mode (Johnson

et al. 2001) from that of the isopods: males are exceedingly rare in samples, probably owing to the short lifetime of non-feeding terminal males. The tanaids show a level of species diversity and abundance (Table 9) that is similar to that of the isopods, but with a different pattern. While isopods had the highest species diversity at site A, tanaids had approximately similar species diversity at both sites A and C (Fig. 12), which is similar to the isopod species diversity at the PRA site. Tanaid species diversity is substantially less than isopods at site A and site C (compare Tables 8 and 9). Because these data are sparse, the total species estimates show a poorer fit to the lognormal distribution. Nevertheless, the bootstrap estimator for total species suggests that site C is more speciose than site A (112 species vs. 86 species, respectively). This result is supported by an ad hoc extension of the rarefaction curves (Fig. 12), for which the site C curve would cross the site A curve if more individuals were in the data.

Fig. 9 Isopoda. Sanders–Hurlbert rarefaction graph for Domes site A, site C, and the PRA site



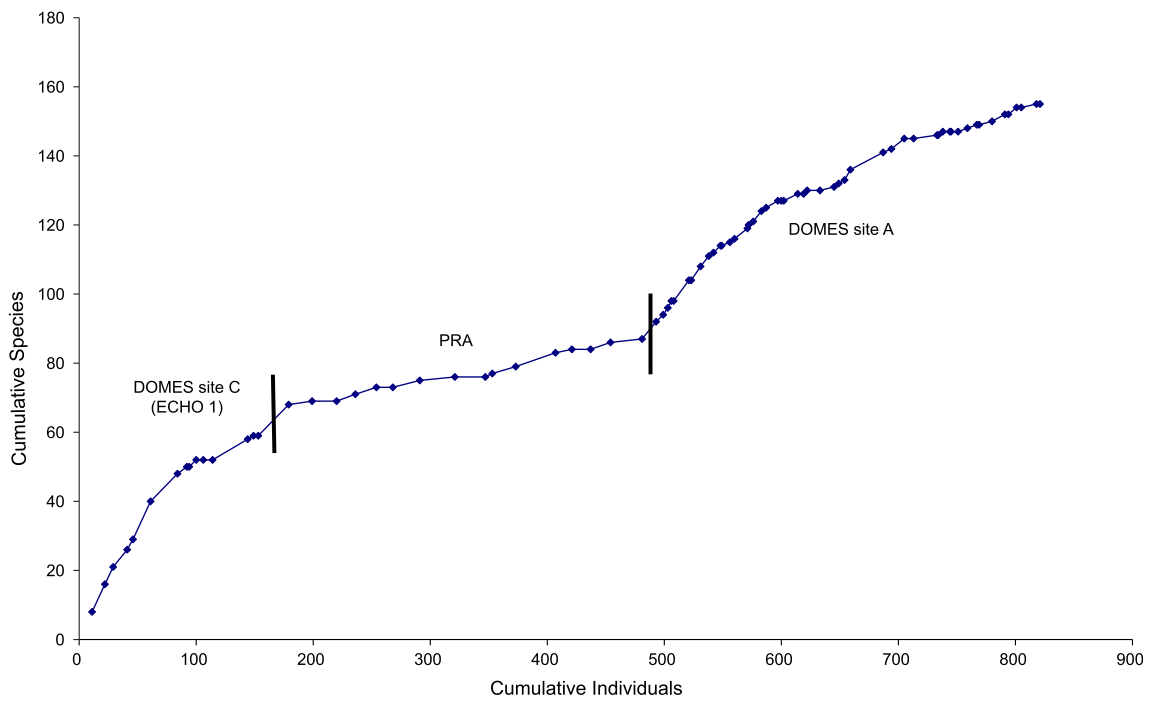


Fig. 10 Isopoda. Species accumulated by individuals, oriented longitudinally east to west

Faunal similarity

The Polychaeta and Isopoda datasets were each pooled by locality and NESS was calculated using the same sample size, $m = 50$, for all taxocenes so the similarities would be comparable (Table 10). The values for the polychaetes and for the isopods are strikingly different, with the former showing similarities of 0.66 to 0.73 over the entire span of distances from 2893

to 357 km, whereas the latter are less than 0.5 even for the relatively nearby pair, Site C to the PRA site (Fig. 13). The single value for the tanaids, Site A – Site C, is shows approximately the same value as the same pair of sites for the polychaetes. This result shows that although data for the isopods and tanaids are smaller compared to the polychaete data, they can nevertheless have distinctly different similarities. These differences have important consequences for the total species

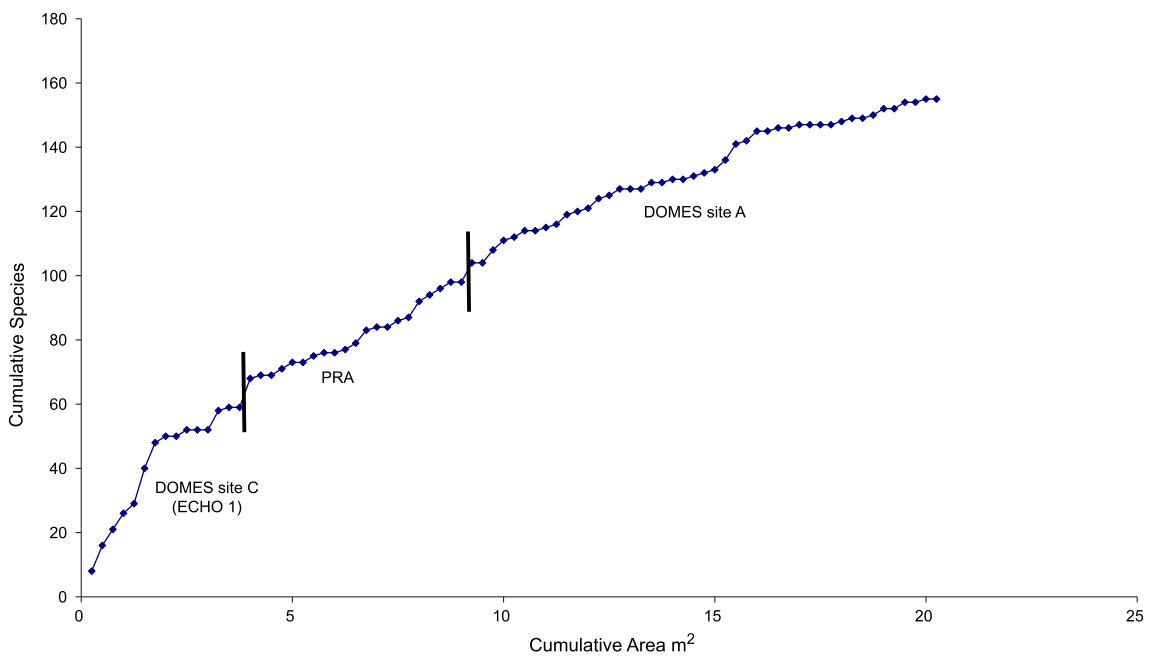
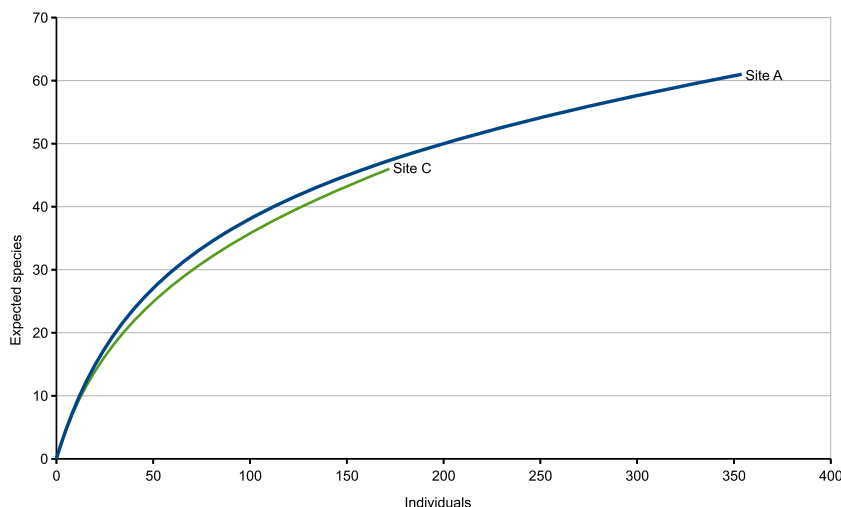


Fig. 11 Isopoda. Species accumulated by area of samples, oriented longitudinally east to west

Fig. 12 Tanaidacea. Sanders–Hurlbert rarefaction graph for DOMES site A and site C



richness of the CCFZ. Because isopod species composition changes with distance at a much higher rate than the polychaetes, i.e. has a higher beta diversity, if integrated across the entire CCFZ, the isopods have a greater numbers of species. The NESS estimator is sensitive to sample size, m , so that as m is higher, the measure becomes more sensitive to the rarer species (Grassle and Smith 1976). If NESS is calculated for the maximum m for each data set (Table 11), the mean polychaete NESS estimate, which had a much higher m_{max} than 50 (317), the mean similarity decreased by 7.72%. The Isopods ($m_{max} = 76$), which had many rare species, actually became somewhat more similar (1.91%) on the average. The single tanaid value ($m_{max} = 86$), which had approximately similar abundances to the isopods, decreased by 3.33%.

Discussion

Sampling taxocenes

These results suggest that, although the data were nearly adequate for the abundant polychaetes, more quantitative samples (more than 15–16 box corer samples) are needed for recovering

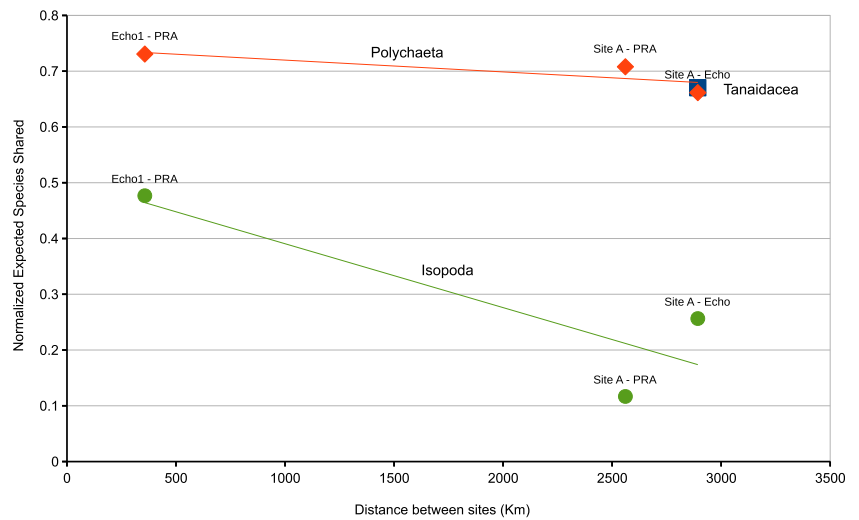
robust estimates of diversity in the isopods or tanaids. This is especially true for the isopods, which had extremely high level of beta diversities relative to the polychaetes. For example, if individuals in the theoretical species abundance distribution (7397 ind) are totaled and divided by the isopod density for Site A (27.02 ind/m²), the approximate minimum area needed to collect the estimated 129 species isopods at Site A is 274 m², which amounts to 1095 box corer samples. For a less diverse habitat like the ECHO I locality at Site A, the same calculation yields 19 m² and a somewhat more achievable number of 76 box corers, which is approximately the same number of samples taken at Site A during the two R/V *Oceanographer* cruises. Increasing the box corer size to 1.0 m² is one approach that has been discussed, but the operation and processing of such large samples becomes impractical, and probably would not result in saved ship time. Clearly, capturing all species is impractical, so working with smaller numbers of samples and using estimation techniques will have to suffice. If the isopods were distributed randomly at Site A, 50 samples should have given a good fit to the lognormal distribution but, because they have a contagious dispersion pattern, more samples might have given a better estimate.

Table 10 Polychaeta, normalized expected species shared(NESS)

Sites	Distance (km)	Polychaeta NESS	Isopoda NESS	Tanaidacea NESS
Site A – Site C	2893	0.662	0.256	0.670
Site A – PRA	2561	0.708	0.117	–
Site C – PRA	357	0.731	0.477	–
Rate of change (species/km)		0.0120	0.0056	–
Species range (km/species)		83.7	179.8	–
Species range (km ² / species)		2,228	10,289	–

Calculations described in Materials and Methods. NESS calculated at sample size $m = 50$ individuals to allow comparison between taxa. Great circle distances to between site pairs are given for comparison. The rate of change (species/km) is the slope of the linear regression in Fig. 13 times the mean total estimated species at all sites (Tables 7, 8, 9)

Fig. 13 Normalized Expected Species Shared ($m = 50$) for Polychaeta and Isopoda plotted against distances between those sites. *Filled diamonds*, Polychaeta; *filled circles*, Isopoda; *filled square*, Tanaidacea, single value. Linear regression, great circle distances separating sites and NESS: Polychaeta, y intercept 0.7410103, slope -0.0000212 ; Isopoda, y intercept: 0.5051448121, slope -0.0001145



Another implication of these results is that combining data for all taxa into single diversity estimates may obscure the patterns that dominate benthic assemblages. In highly species-rich assemblages, the probability of sampling a particular species is low, so many samples are required capture a useful sample of that single species. The other aspect of this problem is that establishing the distribution of any particular species over an arbitrary distance multiplies this problem by however many distinct sites are desired. Although non-quantitative samplers, such as the epibenthic sled, capture large swath of an assemblage, these samplers are notoriously biased in which taxa they capture, and will often miss strongly infaunal taxa; for example, compare Thambematidae abundances between box corers and epibenthic sleds in Harrison (1987). Because of this bias, non-quantitative samplers will also strongly distort species-abundance relationships. On manganese nodule dominated sea floors, sleds are also poor samplers of the nodule epifauna, which often require special handling to assess accurately (Mullineaux 1987).

Diversity and productivity

The polychaete data have been used to assess the influence of surface and export productivity (Paterson et al. 1998; Glover et al. 2002). The isopod data, however, show a different trend

from the polychaete data. The faunal density estimates show the strongest correlation with CHL, although estimated export POC shows the same trend. The bootstrap lognormal estimated total species, on the other hand, varies with regard to POC. The polychaetes show a positive relationship with POC, ranging from 203 total species at site A to 310 species at the PRA site. The isopods have a inconsistently negative relationship to POC. The isopods are especially speciose (143 bootstrap lognormal estimated total species) at the low productivity site A but have many fewer species at the higher productive sites C and PRA (79 and 91 species, respectively). Although habitat heterogeneity might explain the differences (such as sedimentary heterogeneity; Etter and Grassle 1992), sediments, nodule composition and geomorphology are similar across the entire CCFZ (Piper et al. 1979a, b), with the strongest variables being sedimentary rate and productivity. The tanaids, for which only data from sites A and C are available, show a trend similar to that of the polychaetes, with the bootstrap lognormal estimated total species highest at the high POC PRA site (112 species) and lowest at the low POC site A (87 species). Here, diversity is not necessarily related to POC and might even have a negative relationship in the isopods. Despite only having data from three sites, these results are at least indicative and worthy of additional study. These findings are in stark contrast to a recent multi-investigator study (Woolley et al. 2016) which found that export POC

Table 11 Normalized expected species shared(NESS)

Sites	Distance km	Polychaeta NESS	Isopoda NESS	Tanaidacea NESS
m_{max}		317	76	86
Site A – Site C	2893	0.588	0.244	0.648
Site A – PRA	2561	0.653	0.129	–
Site C – PRA	357	0.697	0.493	–

Calculations described in [Materials and Methods](#). NESS calculated at maximum sample size m_{max} for each taxocene. Great circle distances to between site pairs are given for comparison

and proximity to slope habitats drive deep-sea diversity. One might attribute their results to the target of their research, the megafaunal taxocene Ophiuroidea, although they argued that this was a general result for deep-sea assemblages. These results point to the pitfalls of using one taxocene as a proxy for the entire fauna as each group has its own unique ecological and evolutionary response to the deep-sea environment.

Beta diversity and reproductive mode

As proposed by McClain and Rex (2015), beta diversity can be assessed using distance decay methods. Here, this is provided by the slope of a linear regression of the distances and NESS between pairs of sites (Fig. 13; Table 10) and multiplying it by the mean total species richness at all three sites for isopods or polychaetes (Tables 7, 8). Admittedly, these regressions provide a poor match to the data, but they provide an approximate comparison of the beta diversity in polychaetes and isopods. The calculation suggests that isopods change at a rate of 0.012 species per km, and the inverse of which gives an approximate linear species range of 84 km. The much more species rich and abundant polychaetes, on the other hand, change little over greater distances, 0.0056 species per km, so the average species range is 180 km. If this estimate is expanded to an areal estimate, assuming an approximately circular distribution, an isopod species range could be 2,228 km² while a polychaete species range could be 10,289 km². Although the level of species nestedness and species replacement (cf. McClain and Rex 2015) cannot be addressed directly, the low similarity in the isopods between widely separated sites suggests that the main process is species replacement, while the similarity between sites in the polychaetes argues for a higher degree of nestedness, although certainly replacement is also taking place.

The reproductive modes of the two taxocenes may provide an understanding of these differences. Because some polychaetes may have larval dispersal combined with slow development at deep sea temperatures that extends the larval period, each species could maintain connectivity over great distances in the deep sea. Furthermore, modes of reproduction in polychaetes include both sexual and asexual reproduction, which contribute to the reproductive success of each individual. The polychaete result may also be explained as a negative bias owing to our inability to distinguish closely related species (Nygren 2014). If so, polychaete species turnover could be much higher in the CCFZ. The direct developing isopods have no swimming larval dispersal, and can only disperse as adults or juveniles. In addition, isopod species are much more readily identified to

species, owing to their abundance of external morphological features, which allows one to separate members of species flocks such as the northern hemisphere *Eurycope complanata* species complex (Wilson 1983). The rarity of each isopod species might seem to militate against the persistence of the rare species because the probability of encounter for reproductive adults would be extremely low. The reproductive ability of females to mate at an early age and retain sperm until fertilization (Wilson 1991) increases the likelihood of successful reproduction. Additionally, deep-sea species in aggregate show a clumped distribution (Jumars 1976), which also improves the probability of reproductive encounters. Consequently, the range of an isopod species can be quite small, with low connectivity between regions.

The single NESS value for the Tanaidacea at sites A and C implies that this group might have a beta diversity that is similar to the Polychaeta, which runs counter to the idea that Peracarida, in general, should have low connectivity and high beta diversities. Isopods and tanaids, however, differ considerably in their reproductive mode (Johnson et al. 2001). While the isopods have males and females that are fully functional as adults, tanaid terminal males are non-feeding and are highly transformed for locomotion. While sex ratios of isopods are more or less equal, the observed sex ratios of tanaids are highly skewed toward females; males are extremely rare in the DOMES samples (unpublished data). The males are rare in the samples because they are both highly motile and less likely to be sampled, but also because their residence time in the assemblage is short compared to the adult females. These observations imply that the tanaid males might be the agent of connectivity in this otherwise sedentary, largely tubicolous infaunal group (Wilson 1987a, b).

What these beta diversity results mean between the sites where we don't have samples is unknown. We do not have fine-scaled sampling that connects assemblages that are statistically different (using NESS or any other estimator). Unlike shallow water that has a coarse grained physical structure with distance, the deep-sea in the CCFZ is continuous but environmentally varying with distance. Do we have deep-sea connectivity for populations that are genetically linked over long distances by way of continuous replacement of one form with another? Or do we have zones of introgression or even abrupt breaks and well-defined species distributions? Samples at a fine scale over a large distance are needed to answer this question. So, although we might say that one species at site A is different from one at site C, the possibility exists that they are connected but the transition between forms is unobserved. We can discuss connectivity as long as we are clear that we do not know the fine details.

Acknowledgements Peter A. Jumars, Robert R. Hessler and Fred N. Spiess directed the initial NOAA programs and provided much of the intellectual overview to the ongoing programs. The captains, chief engineers, crews, and scientific parties of the research vessels *Melville*, *Oceanographer*, *New Horizon* and *Moana Wave* tirelessly provided their expertise to collect the samples on which this research is based. Taxonomic expertise for the macrofauna was provided by Jurgen Sieg, Kristian Fauchald, Kirk Fitzhugh, Timothy Ragen, and Elana Varnum. Susan Garner and coworkers in my Scripps lab, and Liko Self and coworkers in the Jumars lab at the University of Washington were invaluable in sorting the samples and organizing the large datasets that resulted from the field programs. George Sugihara (SIO) provided the original Fortran of the lognormal estimation algorithm that I extended with a bootstrap estimator. Eugene D. Gallagher (University of Massachusetts, Boston) provided the corrected Fortran NEWNESS program and advised on various analytical issues. I am grateful to Dwight Trueblood, who found Jumars (1980) in his NOAA office files. This research was funded by NOAA contracts 03-78-B01-17, 83-SAC-00659, NA-84-ABH-0300, 40-AANC-701124, 50-DGNC-8-00113, 50-DSNC-9-00108. Two anonymous referees kindly provided helpful advice, who requested clarifications on the methods employed, productivity estimates and probable dispersal modes. I am grateful to these people and institutions for their contributions to this research.

References

- Bischoff JL, Piper DZ (eds) (1979) Marine geology and oceanography of the Pacific manganese nodule province vol 9. Marine Science. Plenum (Springer US), New York
- Blake JA, Arnofsky PL (1999) Reproduction and larval development of the spioniform Polychaeta with application to systematics and phylogeny. *Hydrobiologia* 402:57–106. doi:10.1023/a:1003784324125
- Chao A (1984) Nonparametric estimation of the number of classes in a population. *Scand J Stat* 11:265–270
- Chao A, Chiu C-H (2016) Nonparametric estimation and comparison of species richness. *Els*, pp. 1–11. John Wiley & Sons, Ltd, Chichester
- Cohen AC Jr (1950) Estimating the mean and variance of normal populations from singly truncated and doubly truncated samples. *Ann Math Stat* 21:557–569
- Colwell RK (2013) EstimateS: Statistical estimation of species richness and shared species from samples. Version 9. User's Guide and application published at: <http://purl.oclc.org/estimates>. Accessed 3 Nov 2016
- Colwell RK, Coddington JA (1994) Estimating terrestrial biodiversity through extrapolation. *Philos Trans R Soc Lond B* 345:101–118
- Craig JD (1979) The relationship between bathymetry and ferromanganese deposits in the north equatorial Pacific. *Mar Geol* 29:165–186. doi:10.1016/0025-3227(79)90107-5
- Cunha MR, Wilson GDF (2003) Haplomunnidae (Crustacea: Isopoda) reviewed, with a description of an intact specimen of *Thylakogaster* Wilson & Hessler, 1974. *Zootaxa* 326:1–16
- de Moustier C (1985) Inference of manganese nodule coverage from Sea Beam acoustic backscattering data. *Geophysics* 50:989–1001. doi:10.1190/1.1441976
- Dick RE, Foell EJ (1985) Analysis of SIO deep tow photographs of mining device tracks, “ECHO-1” cruise, mining test site. Deepsea Ventures, Inc., Gloucester Point, Virginia
- Efron B (1979) Bootstrap methods: another look at the jackknife. *Ann Stat* 7:1–26
- Efron B, Gong G (1983) A leisurely look at the bootstrap, the jackknife, and cross-validation. *Am Stat* 37:36–48. doi:10.1080/00031305.1983.10483087
- Etter RJ, Grassle JF (1992) Patterns of species diversity in the deep sea as a function of sediment particle size diversity. *Nature* 360:576–578
- Franke H-D (1999) Reproduction of the Syllidae (Annelida: Polychaeta). *Hydrobiologia* 402:39–55. doi:10.1023/a:1003732307286
- Gardner WD, Sullivan LG, Thorndike EM (1984) Long-term photographic, current, and nephelometer observations of manganese nodule environments in the Pacific. *Earth Planet Sci Lett* 70:95–109. doi:10.1016/0012-821X(84)90212-7
- Glover AG, Smith CR (2003) The deep-sea floor ecosystem: current status and prospects of anthropogenic change by the year 2025. *Environ Conserv* 30:219–241
- Glover AG, Smith CR, Paterson GLJ, Wilson GDF, Hawkins L, Shearer M (2002) Polychaete species diversity in the central Pacific abyss: local and regional patterns, and relationships with productivity. *Mar Ecol Prog Ser* 240:157–170
- Grassle JF, Maciolek NJ (1992) Deep-sea species richness: regional and local diversity estimates from quantitative bottom samples. *Am Nat* 139:313–341
- Grassle JF, Smith W (1976) A similarity measure sensitive to the contribution of rare species and its use in investigation of variation of marine benthic communities. *Oecologia* 25:13–22
- Harrison K (1987) Deep-sea asellote isopods of the north-east Atlantic: the family Thambematidae. *Zool Scr* 16:51–72
- Hayes SP (1979) Benthic current observations at DOMES sites A, B, and C in the tropical central north pacific ocean. In: Bischoff JL, Piper DZ (eds) Marine geology and oceanography of the Pacific manganese nodule province. Plenum Press (Springer US), New York, pp 83–112
- Hecker B, Paul AZ (1979) Abyssal community structure of the benthic infauna of the Eastern equatorial pacific: DOMES sites A, B, and C. In: Bischoff JL, Piper DZ (eds) Marine geology and oceanography of the Pacific manganese nodule province. Plenum (Springer US), New York, pp 287–308
- Hein JR, Mizell K, Koschinsky A, Conrad TA (2013) Deep-ocean mineral deposits as a source of critical metals for high- and green-technology applications: comparison with land-based deposits. *Ore Geol Rev* 51:1–14
- Hessler RR (1993) Swimming morphology in *Eurycope cornuta* (Isopoda: Asellota). *J Crust Biol* 13:667–674
- Hessler RR, Jumars PA (1974) Abyssal community analysis from replicate box cores in the central North pacific. *Deep-Sea Res* 21:185–209
- Hurlbert SN (1971) The nonconcept of species diversity: a critique and alternative parameters. *Ecology* 52:577–586
- Johnson DA (1972) Ocean-floor erosion in the equatorial pacific. *Geol Soc Am Bull* 83:3121–3144. doi:10.1130/0016-7606(1972)83[3121:oeitep]2.0.co;2
- Johnson WS, Stevens M, Watling L (2001) Reproduction and development of marine peracaridans. *Adv Mar Biol* 39:107–220
- Jumars PA (1976) Deep-sea species diversity: does it have a characteristic scale? *J Mar Res* 34:217–246
- Jumars PA (1977) Potential environmental impact of deep-sea manganese nodule mining: community analysis and prediction vol unpublished manuscript no.13. US National oceanic and atmospheric administration. Pacific Marine Environmental Laboratory, Seattle
- Jumars PA (1980) Impact of a pilot-scale manganese nodule mining test on the benthic community Contract No. 03-78-B01-17. Department of Oceanography, University of Washington, Seattle
- Jumars PA (1981) Limits in predicting and detecting benthic community responses to manganese nodule mining. *Mar Min* 3:213–229
- Knoop PA, Owen RM, Morgan CL (1998) Regional variability in ferromanganese nodule composition: northeastern tropical. *Pac Ocean Mar Geol* 147:1–12. doi:10.1016/S0025-3227(97)00077-7

- Lavelle JW, Ozturgut E, Swift SA, Erickson BH (1981) Dispersal and resedimentation of the benthic plume from deep-sea mining operations: a model with calibration. *Mar Min* 3:59–93
- Lutz MJ, Caldeira K, Dunbar RB, Behrenfeld MJ (2007) Seasonal rhythms of net primary production and particulate organic carbon flux to depth describe the efficiency of biological pump in the global ocean. *J Geophys Res Oceans* 112:26. doi:10.1029/2006jc003706
- Martino S, Parson LM (2012) A comparison between manganese nodules and cobalt crust economics in a scenario of mutual exclusivity. *Mar Policy* 36:790–800. doi:10.1016/j.marpol.2011.11.008
- McAleece N, Gage JD, Lambshead PJD, Paterson GLJ (1997) BioDiversity professional statistics analysis software. Scottish Association for Marine Science and the Natural History Museum, London, <http://www.sams.ac.uk/peter-lamont/biodiversity-pro>. Accessed Oct 2016
- McClain CR, Rex MA (2015) Toward a conceptual understanding of beta-diversity. In: Futuyma DJ (ed) *Annual review of ecology, evolution, and systematics*, vol 46, pp. 623–642. doi:10.1146/annurev-ecolsys-120213-091640
- Miljutin DM, Miljutina MA, Arbizu PM, Galéron J (2011) Deep-sea nematode assemblage has not recovered 26 years after experimental mining of polymetallic nodules (Clarion-Clipperton Fracture Zone, Tropical Eastern Pacific). *Deep Sea Res I Oceanogr Res Pap* 58: 885–897. doi:10.1016/j.dsr.2011.06.003
- Morel A, Berthon J-F (1989) Surface pigments, algal biomass profiles, and potential production of the euphotic layer: Relationships reinvestigated in view of remote-sensing applications. *Limnol Oceanogr* 34:1545–1562. doi:10.4319/lo.1989.34.8.1545
- Morgan CL, Odunton NA, Jones AT (1999) Synthesis of environmental impacts of deep seabed mining. *Mar Georesour Geotechnol* 17:307–356. doi:10.1080/106411999273666
- Mudie JD, Grow JA, Bessey JS (1972) A near-bottom survey of lineated abyssal hills in the equatorial Pacific. *Mar Geophys Res* 1:397–411. doi:10.1007/bf00286741
- Mullineaux LS (1987) Organisms living on manganese nodules and crusts: distribution and abundance at three North Pacific sites. *Deep Sea Res A Oceanogr Res Pap* 34:165–184
- Mullineaux LS (1988a) The role of settlement in structuring a hard-substratum community in the deep sea. *J Exp Mar Biol Ecol* 120: 247–261
- Mullineaux LS (1988b) Taxonomic notes on large agglutinated foraminifers encrusting manganese nodules, including the description of a new genus, *Chondrodapis* (Komokiacea). *J For Res* 18:46–53. doi:10.2113/gsjfr.18.1.46
- Mullineaux LS (1989) Vertical distributions of the epifauna on manganese nodules: Implications for settlement and feeding. *Limnol Oceanogr* 34:1247–1262
- Nygren A (2014) Cryptic polychaete diversity: a review. *Zool Scr* 43: 172–183. doi:10.1111/zsc.12044
- Osborn KJ (2009) Relationships within the Munnopsidae (Crustacea, Isopoda, Asellota) based on three genes. *Zool Scr* 38:617–635
- Paterson GLJ, Wilson GDF, Cosson N, Lamont PA (1998) Hessler and Jumars (1974) revisited: abyssal polychaete assemblages from the Atlantic and Pacific. *Deep-Sea Res II Top Stud Oceanogr* 45:225–252
- Piper DZ, Blueford JR (1982) Distribution, mineralogy, and texture of manganese nodules and their relation to sedimentation at DOMES Site A in the equatorial North Pacific. *Deep Sea Res A Oceanogr Res Pap* 29:927–951. doi:10.1016/0198-0149(82)90019-X
- Piper DZ, Cook HE, Gardner JV (1979a) Lithic and acoustic stratigraphy of the equatorial north Pacific: DOMES sites A, B, and C. In: Bischoff JL, Piper DZ (eds) *Marine geology and oceanography of the Pacific manganese nodule province*. Plenum (Springer US), New York, pp 309–348
- Piper DZ, Leong K, Cannon WF (1979b) Manganese nodule and surface sediment compositions: DOMES sites A, B, and C. In: Bischoff JL, Piper DZ (eds) *Marine geology and oceanography of the Pacific manganese nodule province*. Plenum (Springer US), New York, pp 437–474
- Preston FW (1962a) The canonical distribution of commonness and rarity: part I. *Ecology* 43:185–215. doi:10.2307/1931976
- Preston FW (1962b) The canonical distribution of commonness and rarity: Part II. *Ecology* 43:410–432. doi:10.2307/1933371
- Quinterno P, Theyer F (1979) Biostratigraphy of the equatorial north Pacific: DOMES sites A, B, and C. In: Bischoff JL, Piper DZ (eds) *Marine Geology and oceanography of the Pacific manganese nodule province*. Plenum (Springer US), New York, pp 349–364
- Riehl T, Wilson GDF, Malyutina MV (2014) Urstylidae – a new family of abyssal isopods (Crustacea: Asellota) and its phylogenetic implications. *Zool J Linn Soc* 170:245–296. doi:10.1111/zoj.12104
- Sanders HL (1968) Marine benthic diversity: a comparative study. *Am Nat* 102:243–282
- Smith KL, Ruhl HA, Kahru M, Huffard CL, Sherman AD (2013) Deep ocean communities impacted by changing climate over 24 y in the abyssal northeast. *Pac Ocean Proc Natl Acad Sci* 110:19838–19841. doi:10.1073/pnas.1315447110
- Spieß FN, Weydert M (1987) Operational aspects, geology and physical effects of dredging. In: Spiess FN, Hessler RR, Wilson GDF, Weydert M (eds) *Environmental effects of deep-sea dredging (final report to the national oceanic and atmospheric administration on contract NA83-SAC-00659)*, vol SIO Reference 87-5. Scripps Institution of Oceanography, La Jolla, pp 1–23
- Spieß FN, Hessler R, Wilson G, Weydert M, Rude P (1984) ECHO I cruise report vol 84-3. Scripps Institution of Oceanography, La Jolla. doi:10.13140/RG.2.1.4131.0242
- Sugihara G (1980) Minimal community structure: an explanation of species abundance patterns. *Am Nat* 116:770–787
- Thiel H (1983) Meiobenthos and nanobenthos of the deep sea. In: Rowe GT (ed) *The sea*, vol 8. Wiley, New York, pp 167–230
- Thistle D, Wilson GDF (1987) A hydrodynamically modified, abyssal isopod fauna. *Deep-Sea Res* 34:73–87. doi:10.1016/0198-0149(87)90123-3
- Thistle D, Wilson GDF (1996) Is the HEBBLE isopod fauna hydrodynamically modified? A second test. *Deep-Sea Res Part A Oceanogr Res Pap* 43:545–554
- Wilson GDF (1983) Systematics of a species complex in the deep-sea genus *Eurycope*, with a revision of six previously described species (Crustacea, Isopoda, Eurycopidae). *Bull Scripps Inst Oceanogr* 25: 1–64
- Wilson GDF (1987a) Crustacean communities of the manganese nodule province. Scripps Institution of Oceanography, La Jolla. doi:10.13140/RG.2.1.4645.0729
- Wilson GDF (1987b) Differences in dispersal and speciation between deep-sea tanaids and isopods (Crustacea). *Am Zool* 23:140A
- Wilson GDF (1989) A systematic revision of the deep-sea subfamily Lipomerinae of the isopod crustacean family Munnopsidae. *Bull Scripps Inst Oceanogr* 27:1–138
- Wilson GDF (1990a) Manganese nodule mining impact studies: *RUM 3 – R/V New Horizon Cruise “QUAGMIRE II”*: 23 April - 17 May 1990. Post Cruise Rep SIO Ref Ser 90:1–43
- Wilson GDF (1990b) Biological evaluation of a preservational reserve area “BEPRA I”; cruise report and interim report on laboratory analysis. An oceanographic cruise from Puntarenas, Costa Rica to Honolulu, Hawaii on the R/V Moana Wave (University Of Hawaii) during 22 September To 14 October, 1989 SIO Ref Ser 90:1–34
- Wilson GDF (1990c) The biological impact of deep ocean manganese nodule mining - a review of current programs and future directions. Report on a Workshop held on July 6-7, 1989 at the Scripps Institution of Oceanography SIO Ref Ser 90:1–73. doi:10.13140/RG.2.1.2417.5521

- Wilson GDF (1991) Functional morphology and evolution of isopod genitalia. In: Bauer RT, Martin JW (eds) *Crustacean sexual biology*. Columbia University Press, New York, pp 228–245
- Wilson GDF (1992) Biological evaluation of a preservational reserve area; faunal data and comparative analysis. Australian Museum, Sydney. doi:[10.13140/RG.2.1.2416.8484](https://doi.org/10.13140/RG.2.1.2416.8484)
- Wilson GDF, Hessler RR (1987) The effects of manganese nodule test mining on the benthic fauna in the North equatorial pacific. In: Spiess FN, Hessler RR, Wilson GDF, Weydert M (eds) *Environmental effects of deep-sea dredging*. Final report to the national oceanic and atmospheric administration on contract NA83-SAC-00659, vol SIO Reference 87–5. SIO Reference, vol 87. Scripps Institution of Oceanography, La Jolla, pp 24–86. doi:[10.13140/RG.2.1.1024.2080](https://doi.org/10.13140/RG.2.1.1024.2080), appendices A-H
- Woolley SNC et al (2016) Deep-sea diversity patterns are shaped by energy availability. *Nature* 533:393–396. doi:[10.1038/nature17937](https://doi.org/10.1038/nature17937)
- Young CM (2003) Reproduction, development and life history traits. In: Tyler PA (ed) *Ecosystems of the deep oceans*. *Ecosystems of the world*, vol 28. Elsevier, Amsterdam, pp 381–426